

4

DTIC FILE COPY

AD-A190 129

OFFICE OF NAVAL RESEARCH

TECHNICAL REPORT

for

1 August 1985 through 31 July 1987

for

Contract N00014-85-K-0555

R&T No. 414e339

DTIC  
ELECTE  
S JAN 13 1988 D  
D

Fundamental Properties and Devices Applications of Ge<sub>x</sub>Si<sub>1-x</sub>/Si Superlattices

Kang L. Wang

University of California, Los Angeles  
405 Hilgard Avenue  
Los Angeles, CA 90024

Reproduction in whole, or in part, is permitted for any purpose of the United States Government.

\* This document has been approved for public release and sale; its distribution is unlimited.

## Table of Contents

1.	Introduction.....	1
2.	Progress.....	3
	(a) Growth and Characterization of $\text{Ge}_x\text{Si}_{1-x}/\text{Si}$ Heterostructures.....	3
	(b) Power Loss of Holes in $\text{Ge}_x\text{Si}_{1-x}/\text{Si}$ Heterostructures.....	6
	(c) Intrasubband Absorption.....	9
	(d) Doping and Impurities in MQW's.....	14
3.	Summary.....	16
4.	References.....	17
5.	Publications as a result of ONR funding.....	18
6.	Appendices.....	21

Accession For	
NTIS CRA&I	<input checked="" type="checkbox"/>
DTIC TAB	<input type="checkbox"/>
Unannounced	<input type="checkbox"/>
Justification	
By	
Date	
Availability Codes	
Dist	Avail and/or Special
A-1	



## ABSTRACT

The progress include (a) growth and characterization of  $\text{Ge}_x\text{Si}_{1-x}/\text{Si}$  epitaxial films and superlattices, (b) study of power loss by two dimensional holes in coherently strained  $\text{Ge}_x\text{Si}_{1-x}/\text{Si}$  heterostructures, (c) theoretical prediction of resonances of intraband absorption (d) study of  $\text{B}_2\text{O}_3$  as a low temperature p-type dopant. Initial stage of growth of  $\text{Ge}_x\text{Si}_{1-x}/\text{Si}$  films were studied using reflection high energy electron diffraction (RHEED) and the superlattice structures were characterized using TEM. In the study of magneto-transport of holes in  $\text{Ge}_x\text{Si}_{1-x}/\text{Si}$  SLS's, we found that the power loss data can be well understood by taking into account the effects from the acoustic mode phonons by both the deformation potential and the piezoelectric coupling. The resonance nature of intraband absorption can be used for sensitive and tunable IR detector applications. We have demonstrated the possibility of using  $\text{B}_2\text{O}_3$  as an effective p-type doping source for providing abrupt doping profiles needed for  $\text{Ge}_x\text{Si}_{1-x}/\text{Si}$  superlattices.

## 1. INTRODUCTION

In the following sections, we will describe the progress of both experimental and theoretical studies of the fundamental properties of  $\text{Ge}_x\text{Si}_{1-x}/\text{Si}$  epitaxial films and superlattices. Various in-situ surface cleaning techniques were investigated using reflection high energy electron diffraction (RHEED). It is essential to find the optimum conditions for surface cleaning prior to MBE growth in order to obtain high quality epitaxial films. We have also used RHEED to monitor the initial stage of the growth of  $\text{Ge}_x\text{Si}_{1-x}$  films on Si(100) and Si(111) substrates.  $\text{Si}/\text{Ge}_x\text{Si}_{1-x}$  superlattices were successfully grown on Si

substrates and characterized by using TEM and Raman spectroscopy. The interface properties were studied using electron energy loss spectroscopy (EELS) and high resolution phonon spectra of  $\text{Ge}_x\text{Si}_{1-x}/\text{Si}$  have also been obtained. Power loss by two dimensional holes in coherently strained  $\text{Ge}_x\text{Si}_{1-x}/\text{Si}$  heterostructures was investigated using hot carrier Shubnikov-de Hass (SdH).

Further, we have begun the investigation of the device applications using  $\text{Ge}_x\text{Si}_{1-x}$ . Theoretical calculations shows the possibility of use of these structures for tunable infrared detectors and sources. New devices due to further the reduction of dimension will also be discussed.

Another area of progress is in doping control. In Si MBE, Sb and Ga are usually thermally-evaporated as n- and p-type dopants, respectively. However, they are found to exhibit low incorporation ratios, i.e., low ratios of dopant concentration in the grown film to the corresponding surface adlayer. We have demonstrated the use of  $\text{B}_2\text{O}_3$  as a low temperature p-type dopant for  $\text{Ge}_x\text{Si}_{1-x}/\text{Si}$  heterostructures.

Detailed of these can be referred to the published papers in the form of preprints and reprints whose abstracts are attached in the appendix.

Meanwhile, UCLA has established an Integrated Si and III-V Compound MBE Laboratory, where combination of Si and III-V superlattices can be grown without breaking the vacuum. We have also setup a magneto-resistance measurement system at our laboratory for further investigation of properties of epitaxial films.

## 2. PROGRESS

### (a) Growth and Characterization of $\text{Ge}_x\text{Si}_{1-x}/\text{Si}$ Heterostructures

In this investigation, the in-situ substrate cleaning techniques were studied [1] to optimize the cleaning conditions in order to obtain high quality epitaxial  $\text{Ge}_x\text{Si}_{1-x}$  films. Prior to loading the samples into the growth chamber, Si substrates were chemically pre-cleaned by the Shiraki method ( $\text{HNO}_3$ ,  $\text{NH}_4\text{OH}$  and  $\text{HCL}$ ). Then the protective oxide film was removed in-situ by (a) thermally heating the substrate (b) depositing a thin film ( $\sim 15 \text{ \AA}$ ) of Si at low flux rates (self-cleaning). In the case of thermal cleaning as the oxide layer is evaporated a sharp mixture of (2X1) and (1X2) RHEED patterns was observed for Si(100) substrates (see Fig. 1 (a)), while a (7X7) reconstruction appeared for Si(111) (see Fig. 1 (b)) at about  $950^\circ\text{C}$ . These are typical reconstruction patterns for the clean Si(100) and Si(111) surfaces. For Si flux cleaning the best RHEED patterns were obtained with a Si flux of  $2 \times 10^{13} \text{ cm}^{-2}\text{s}^{-1}$  at substrate temperature  $800^\circ\text{C}$  and for deposition about 3 minutes.

At the initial stage of the growth of  $\text{Ge}_x\text{Si}_{1-x}$  films on Si(111), there is a sharp transition of RHEED pattern from (7X7) to (5X5). As the film becomes thicker, the (5X5) pattern changes back to (7X7) [2]. We believe that this transition is due to the relaxation of the strain present in the  $\text{Ge}_x\text{Si}_{1-x}$  film. As the film gets thicker the strain is relaxed due to the generation of misfit dislocations at the interface. Further study is currently underway to investigate this phenomenon in detail.

Here we show the characteristics of the growth of extremely thin  $\text{Ge}_x\text{Si}_{1-x}/\text{Si}$  MQW's and SLS's. The Si/ $\text{Ge}_x\text{Si}_{1-x}$  superlattices grown at  $580^\circ\text{C}$

(a)



(b)



Fig. 1. RHEED patterns for SiGe films grown on (a) Si(111) substrate, (b) Si(100) substrate.



Fig. 2 TEM image of a  $\text{Ge}_x\text{Si}_{1-x}/\text{Si}$  superlattice grown on a SOI structure.

$^{\circ}\text{C}$  showed good surface morphology and the TEM pictures indicated the layered structure with uniform film thicknesses as shown in Fig. 2. Fig. 3 illustrates the Auger depth profile of such a superlattices. The strain present in the epitaxial layers were estimated from the peak shifts of the Raman spectrum [4].

The interface properties are also being investigated using electron energy loss spectroscopy (EELS). High resolution phonon spectra have been obtained in collaboration with Professor Lucas in Belgium.

(b) Power Loss of Holes in  $\text{Ge}_x\text{Si}_{1-x}/\text{Si}$  Heterostructures

We have used (in collaboration with the Bell Laboratories) the hot carrier Shubnikov-de Haas (SdH) effect to measure the power loss by hot two-dimensional holes confined near a  $\text{Ge}_{0.2}\text{Si}_{0.8}/\text{Si}$  heterointerface [5,6]. The dependence of carrier temperature on electric field was determined for field strengths between 1.8 mV/cm and 2.5 V/cm, and carrier temperatures between 1.75 $^{\circ}\text{K}$  and 4.2 $^{\circ}\text{K}$ . The dependence of the SdH oscillation amplitude on carrier temperatures is illustrated in Fig. 4. The present modulation doped structures consists of a single wide quantum well ( $\sim 500 \text{ \AA}$ ) having a typical mobility  $\mu_n \sim 3300 \text{ cm}^2/\text{V-s}$  and sheet charge density  $n \sim 5 \times 10^{11} \text{ cm}^{-2}$ . The measured power loss versus carrier temperature data are best described by the two-dimensional formalism of Price assuming negligible screening. Excellent agreement of the theory with the experimental result is obtained only if scattering of the acoustic mode phonons by both the deformation potential and the piezoelectric coupling mechanisms are taken into consideration. The result is shown in Fig. 5. We were therefore able to deduce a value for the piezoelectric constant for  $\text{Ge}_{0.2}\text{Si}_{0.8}$  ( $e_{pz}^2 =$

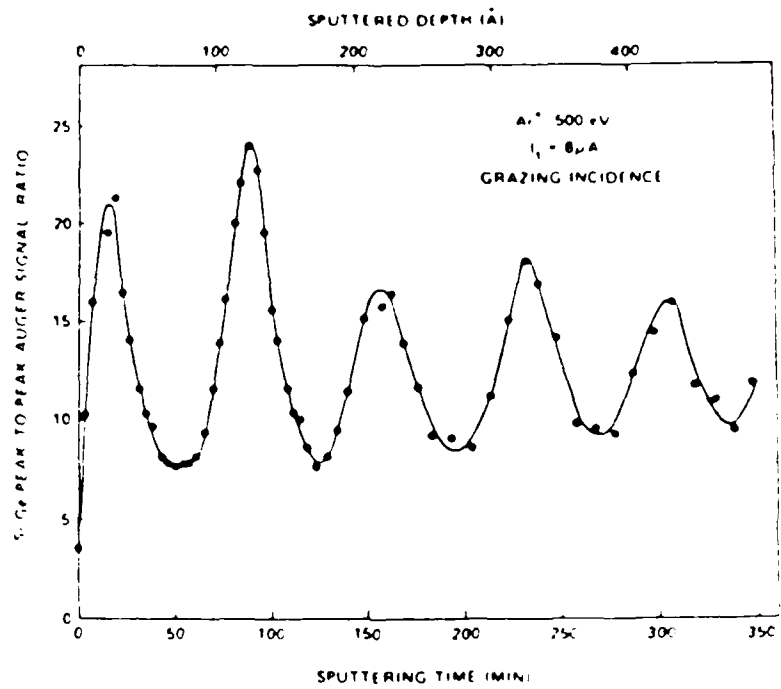


Fig. 3 Auger compositional depth profile of a  $\text{Ge}_x\text{Si}_{1-x}/\text{Si}$  superlattice.

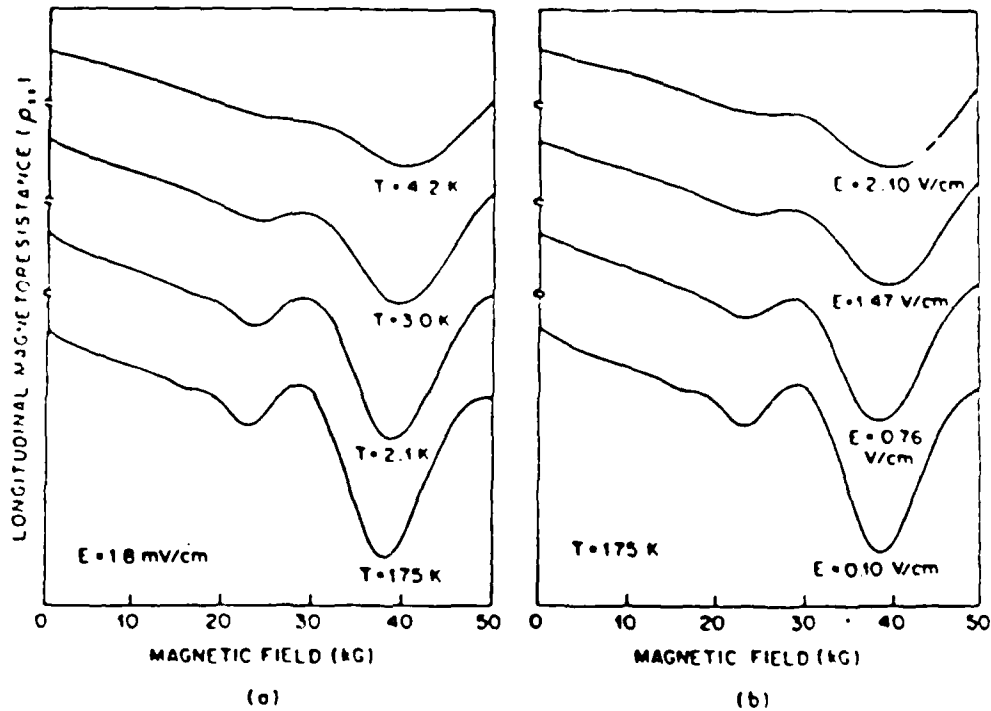


Fig. 4 Amplitude of SdH oscillations (a) at  $E=1.8$  mV/cm for selected temperatures, and (b)  $T_L=1.75$  K for selected electric fields.

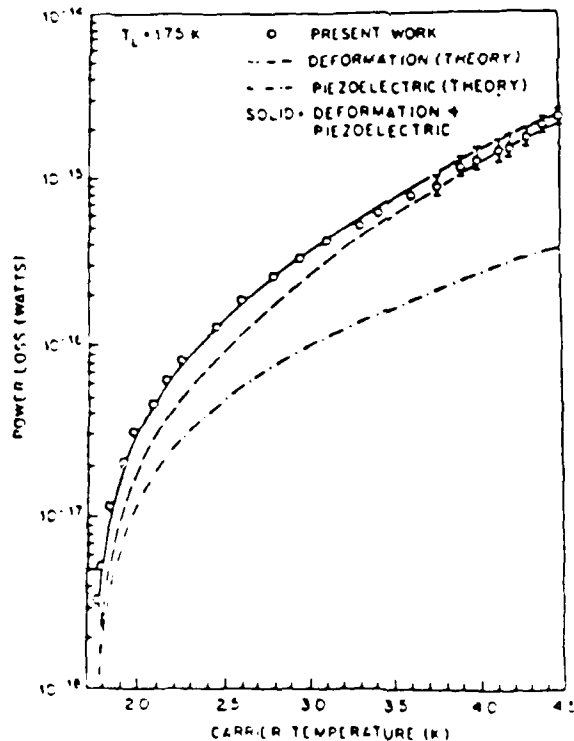


Fig. 5 Open circles give measured power loss vs. carrier temperature. The lower (dot-dashed) curve corresponds the piezoelectric contribution as calculated using Price's formula. The middle (dashed) curve gives the calculated deformation potential contribution (take  $E_{ae} \approx 2.3$ ). The solid curve is the sum of the two (dashes and dot-dashed curves).

$0.16 \times 10^8$  dyne/cm<sup>2</sup> about 30% of that of InAs) which is under coherent strain. The observation of the piezoelectric effect in these otherwise non-piezoelectric structures is attributed to two possible sources:

- (i) lifting of crystalline symmetry due to strain,
- (ii) possible non-randomness of the alloy.

(c) Intraband Absorption

Our recent calculation result of intraband absorption in quantum wells and superlattices suggests tunable detection of electromagnetic waves in a wide range of wavelengths (particular near 10  $\mu$ m) [7]. The subband energy may be written

$$E_n(k) = E_n(0) + \frac{\hbar^2 k_{\perp}^2}{2m_{\perp}^*} + (-1)^n \frac{\hbar^2 q^2}{2m_n^*}$$

where  $k_{\perp}$  is the crystal momentum vector perpendicular to the MQW direction,  $E_n(0)$  is the subband energy at the zone center, and  $k_{\perp}$  and  $q$  are the crystal momentum vector perpendicular and parallel to the MQW directions. The band diagrams for these directions are shown in Fig. 6 (a) and (b), respectively. It is important to recognized that the bands are displaced with a constant value in the  $k_{\perp}$  direction.

Unlike the bulk and interband cases, where transitions occur from the valence subbands to conduction subbands, the intraband transition rates within the conductor band and valence band in MQW's are independent of  $k_{\perp}$  and is shown to be for the first two subbands,

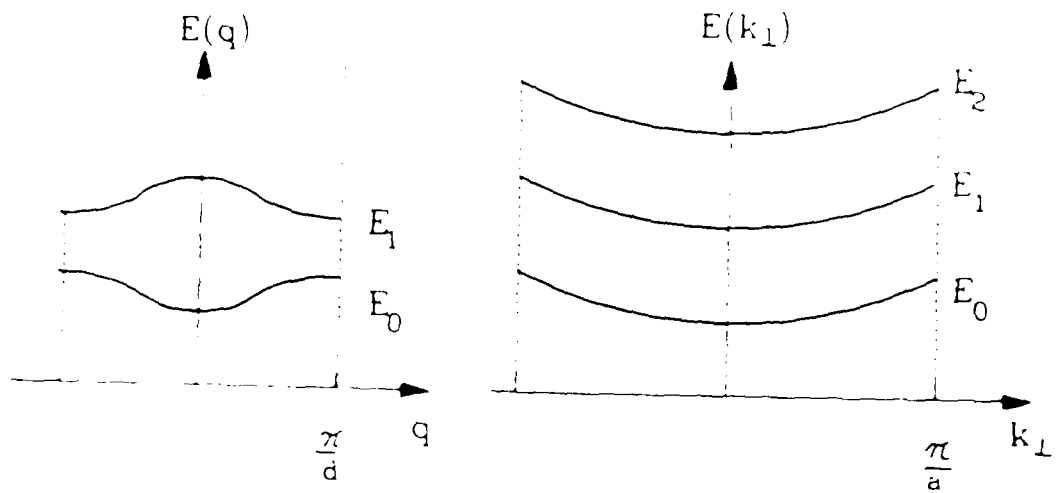


Fig. 6 (a) Energy band in the direction along the MQW direction  
 (b) band perpendicular MQW direction, showing that the difference of the subband energies is independent of  $k_{\perp}$ .

$$E_1 - E_0 = E_1(0) - E_0 + \frac{\hbar^2 q^2}{2m_{mn}^*}$$

where 
$$\frac{1}{m_{mn}^*} = \frac{1}{m_m^*} + \frac{1}{m_n^*} .$$

The general optical absorption is,

$$\alpha(\omega) = \frac{4\pi^2 e^2}{n c m^2} \sum_{\text{BZ}} \frac{2dk}{(2\pi)^3} |e \cdot M_{mn}(h)|^2 \delta[E_m(k) - E_n(k) - \hbar\omega]$$

$$dk = dk_{\perp} dq$$

Where  $M_{mn}$ , the transition matrix of the two subbands can be considered as a smooth function of  $k$ , except at some special points. Then  $\alpha(\omega)$  is proportional to the joint density of states, defined

$$J_{mn}(\hbar\omega) = \int_{\text{BZ}} \frac{2dk}{(2\pi)^3} \delta [ E_m(k) - E_n(k) - \hbar\omega ]$$

or in our case of intraband transitions in SLS's, we have

$$J_{mn} = \frac{k_{\perp}^2}{2(2\pi)} \frac{1}{\nabla_q [ E_m(q) - E_n(q) ]}$$

Consequently, there exist resonances in the optical absorption at the extrema of the subbands when  $\nabla_q E(q) = 0$ . These resonances can be used for sensitive and tunable detectors although the resonance width and thus the quantitative sensitivity still remain to be worked out. It should be recognized that we have ignored the broadening effects due to phonons and impurities. Thus the practical resonance width will be

reduced. Additionally, the carrier lifetimes in the subbands will have to be investigated.

We have also formulated the interband electro-absorption [8,9] and shown an interesting nonlinear effect as illustrated in Fig. 7 in the case of direct gap material AlGaAs/GaAs. The result shows an initial increase of the absorption coefficient at low field and decreases as the electric field exceeds  $75 \text{ KV cm}^{-1}$ . Further confinement of a two-dimensional electron gas, i.e., one-dimensional quantization, can result high speed devices and extremely sensitive photodetectors. A novel one-dimensional electron gas Field Effect Transistor (FET) is proposed [10] with the advantages of higher electron mobility and higher carrier concentration than conventional two-dimensional electron gas FET (TEGFET). Assuming that only the ground subband is occupied, the mobility at low temperature can be approximated as

$$\mu_{1-D} = \frac{e\tau_m(E_F)}{m^*} = \frac{e}{m^*} \left[ \frac{32m^*e^4}{h^3E^2} \frac{N_i}{n_{1-D}} \frac{K_0^2(\pi n_{1-D}r_0)}{\left[1 + \frac{1}{\pi} K_0(\pi n_{1-D}L_1)S_1\right]^2} \right]^{-1} \quad (\text{for line impurity})$$

and

$$\mu_{1-D} = \frac{e}{m^*} \left[ \frac{32m^*e^4}{h^3E^2} \frac{1}{n_{1-D}} \frac{\iint N_0(x,y) K_0^2(\pi n_{1-D} \sqrt{x^2 + y^2}) dy dx}{\left[1 + \frac{1}{\pi} K_0(\pi n_{1-D}L_1)S_1\right]^2} \right]^{-1} \quad (\text{for distributed impurity})$$

where  $k_F = \frac{\pi n_{1-D}}{2}$  is used and  $n_{1-D}$  (Coul/cm) is the 1-D carrier

concentration. The low field mobility for the line charge and distributed charge cases are shown in Fig. 8. Also given in the figure is the 2-D HEMT mobility for comparison. It shows that the low-field mobility of the QWW-HEMT is several orders of magnitude higher than that

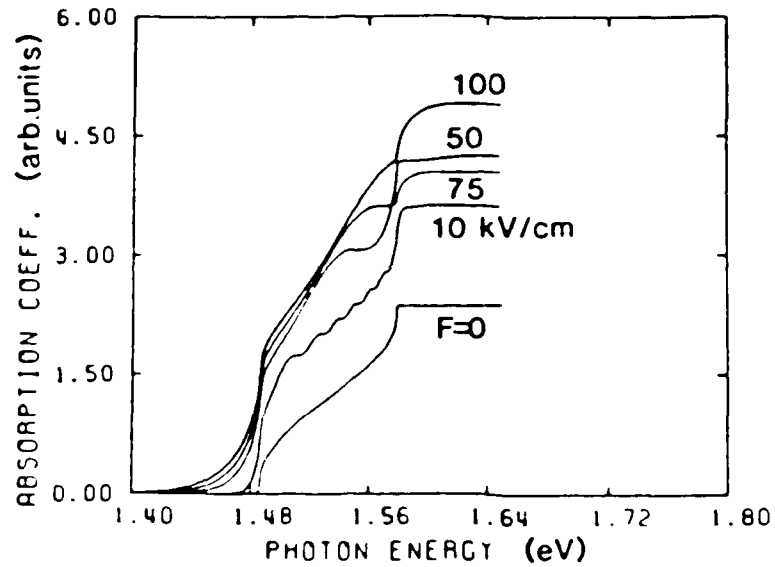


Fig. 7 Absorption coefficient as a function of  $h\nu$  for a superlattice of well and barrier widths 50 and 20 Å respectively.

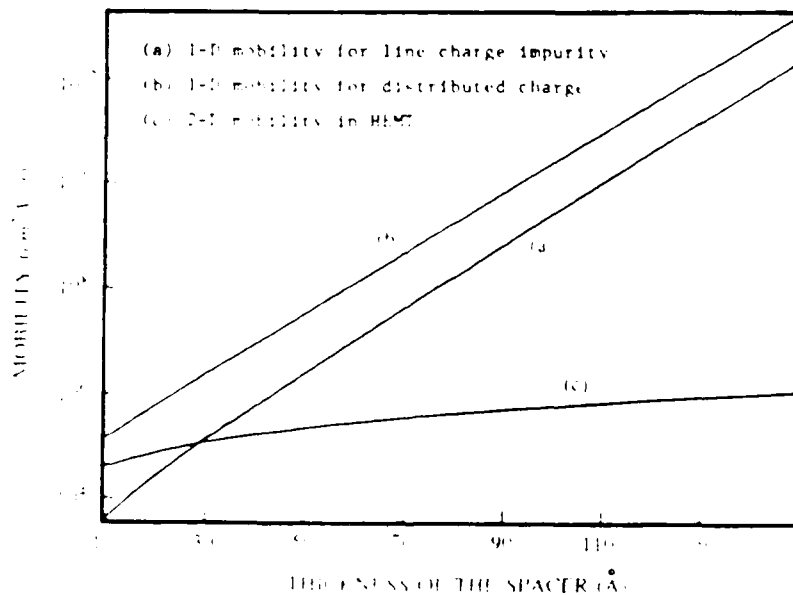


Fig. 8 Comparison of low field mobility due to impurity scattering in low temperature. With the same structure, line(a) for a line charge impurity as done in [3] except the screening effect is also included in our case; (b) for distributed line charge; (c) for the 2-D electron gas in HEMT. The parameters used are:  $d_2$  (thickness of n-AlGaAs) = 30nm,  $r_0$  (thickness of the spacer) from 1nm to 15nm,  $n_{2-D} = 10^{12}/\text{cm}^2$ ,  $L_1 = 10\text{nm}$ ,  $n_{1-D} = n_{2-D} \times L_1 \approx 2 \times 10^6/\text{cm}$ ,  $m^* = 0.067 m_0$ ,  $\epsilon = 12.5 \epsilon_0$ .

in the conventional 2-D HEMT when the thickness of the spacer is large, ignoring phonon scattering.

(d) Doping and Impurities in MQW's

We investigated the possible use of a low temperature boron source using decomposition of  $B_2O_3$  on Si. The undesired oxygen incorporation is reduced during growth. In this study, we demonstrated the possibility of using  $B_2O_3$  as an effective p-type doping source for providing abrupt doping profiles needed for superlattices [11,12]. We find the following: (1) When oxygen is present, it is associated essentially to  $SiO_2$  and  $B_2O_3$ . (2)  $B_2O_3$  is reduced by Si to form  $SiO_2$  and boron incorporated in Si. (3)  $B_2O_3$  reduction is thermally activated for  $T > 500$  °C and the activation energy has been calculated to be  $E_a = 3.0 + 0.5$  eV. For  $T_s > 500$  °C,  $SiO_2$  decomposes into SiO which subsequently desorbs. (4) For  $T_s < 500$  °C, no chemical reaction occurs between Si and  $B_2O_3$ . A typical Auger spectrum, recorded for the experimental condition of  $J_{Si} = 1$  A/min and growth temperature at 690 °C, is shown in the inset of Fig. 9. From these spectra, atomic fractions of the reaction species, Si, Si oxide, O, have been plotted as a function of the silicon flux and are shown in Fig. 9. With this study, we learned how to control boron doping using a  $B_2O_3$  source. Fig. 10 shows a SIMS profile of the abrupt doping distribution accomplished using this source.

With control of doping, it is now possible to explore doping impurities in a very narrow quantum well for IR detection near 10  $\mu$ m. The Hamiltonian for a 2-D hydrogenic impurities in a MQW with the effective mass approximation, may be written

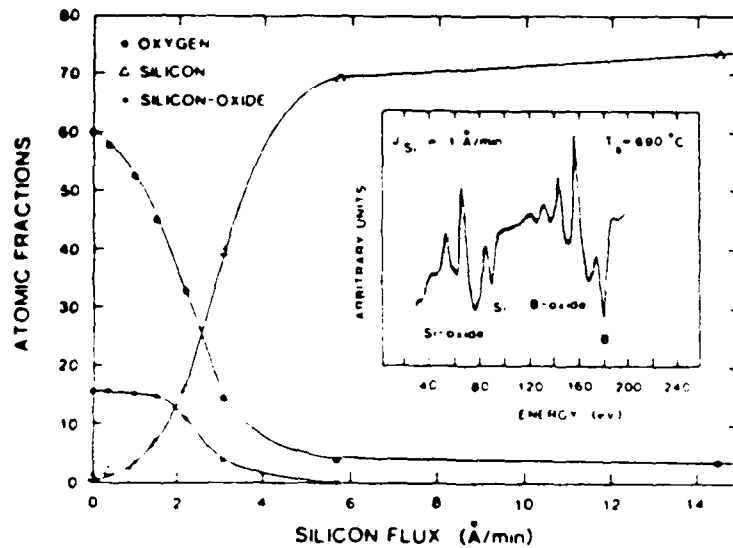


Fig. 9 Evolution of the Si, Si oxide and O atomic fractions in function of the silicon flux ( $0 < J_{Si} < 14.5$  A/min). The growth temperature ( $T_s = 690^\circ\text{C}$ ) and the boron oxide flux ( $J_B = 0.6$  A/min) were kept constant. Inset: Auger Spectrum, taken for  $J_{Si} = 1$  A/min, showing the Si oxide (76 eV), Si (92 eV), B oxide (171 eV) and B (182 eV) transitions.

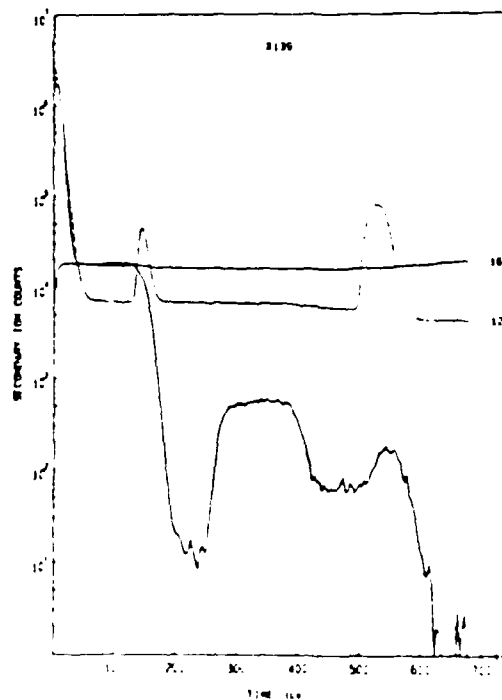


Fig. 10 Secondary ion mass spectroscopy analysis of a boron doped MBE sample using  $\text{B}_2\text{O}_3$ .

$$H = \frac{p^2}{2m^*} - \frac{e^2}{\epsilon_s [p^2 + (z-z_1)^2]^{\frac{1}{2}}} + V(z)$$

$$p^2 = x^2 + y^2$$

where  $z$  is the growth direction and  $V(z)$  is the quantum well potential function and other symbols have their usual meanings. The confinement of the impurities in a MQW can alter the ionization energy, which can be controlled by changing the well width and barrier height. Hence it provides a tunable optical detection wavelengths for application in extrinsic infrared detectors. New physical properties resulting from quantum confinement are extremely important for further understanding and exploitations for device applications. The subsequent work will in part be focused on these areas of research.

### 3. SUMMARY

In summary, the initial stage of growth of  $\text{Ge}_x\text{Si}_{1-x}/\text{Si}$  epitaxial layers and superlattices were investigated using RHEED, TEM, Raman spectroscopy. The possibility of  $\text{B}_2\text{O}_3$  as a low temperature dopant source was studied in order to obtain sharp doping profiles for  $\text{Ge}_x\text{Si}_{1-x}/\text{Si}$  quantum wells and superlattices. We have also measured the electrical characteristics of doped  $\text{Ge}_x\text{Si}_{1-x}$  heterojunctions. New device concepts using the confinement of carriers in quantum wells and superlattices were explored for high speed devices as well as IR detectors and light sources. The subsequent research will focus on testing these concepts and exploration of the additional new properties of these quantum wells and superlattices.

#### 4. REFERENCES

1. T. W. Kang, C. F. Huang, R. P. G. Karunasiri, J. S. Park, C. H. Chern, and K. L. Wang, "Reflection High-Energy Electron Diffraction Observation of Substrate Cleaning During Silicon Molecular Beam Epitaxy", 2nd International Symposium on Silicon Molecular Beam Epitaxy, Hawaii, October 18-23, (1987).
2. T. W. Kang, C. F. Huang, R. P. G. Karunasiri, J. S. Park, and K. L. Wang, "Rheed Studies of MBE-Grown  $\text{Ge}_x\text{Si}_{1-x}$  on Silicon", to appear in J. of Vac. Sci. & Tech. B, (1987).
3. T. W. Kang, J. S. Park, C. F. Huang, R. P. G. Karunasiri, C. H. Chern and K. L. Wang, "Surface Reconstruction of  $\text{Ge}_x\text{Si}_{1-x}$  Observed after Thermal Treatment", MRS Fall Meeting, Boston, (1987).
4. S. J. Chang, M. A. Kallel, and K. L. Wang, "Strain Distribution of MBE Grown  $\text{Ge}_x\text{Si}_{1-x}/\text{Si}$  Layers by Raman Scattering", submitted to SPIE meeting, Spring (1988).
5. Y. H. Xie, R. People, J. C. Bean, and K. W. Wecht, "Power Loss by Two-Dimensional Holes in Coherently Strained  $\text{Ge}_x\text{Si}_{1-x}/\text{Si}$  Heterostructures: Evidence for Weak Screening.", Appl. Phys. Lett. 49, 283 (1986)
6. Y. H. Xie, R. People, J. C. Bean, and K. Wecht, "Investigation on Energy Loss Mechanisms in MBE-Grown  $\text{Ge}_x\text{Si}_{1-x}/\text{Si}$  heterostructure Using Shubnikov-de Haas Effect", the Seventh Molecular Beam Epitaxy Workshop, Massachusetts Institute of Technology, October 20-22, (1986).
7. B. Jogai, and K. L. Wang and J. Schulman, "Intraband Optical Transitions in Superlattices.", to be submitted to Phy. Rev. B15., (1987).
8. B. Jogai, and K. L. Wang, "Interband Optical Transitions in GaAs/GaAlAs Superlattices in an Applied Electric Field," Phy. Rev. B15., January 15, (1987).
9. Jogai, B., and Wang, K. L., "Sensitivity of the Absorption Edge to the Applied Electric Fields in GaAs-GaAlAs Superlattices", to appear in Phys. Rev. Lett., (1987).
10. P. F. Yuh, and K. L. Wang, "One Dimensional Transport in QWW-HEMT", Appl. Phys. Lett., 49(25), 1738, December (1986).
11. E. de Frésart, K. L. Wang, and S. S. Rhee, "Auger Spectrometry and Scanning Electron Microscopy Study of the Interaction of  $\text{B}_2\text{O}_3$  with Silicon Surface," to appear in J. of Vac. Sci. & Tech., (1987).
12. E. de Frésart, K. L. Wang, S. S. Rhee, E. F. Gorey and W. M. Arienzo, "Evaluation of Boron-Doped Si Epilayers Grown by MBE", submitted to Journal of Vacuum Science and Technology (1987).

## 5. PUBLICATIONS RESULTED FROM THE ONR-SUPPORTED RESEARCH

Jogai, B., Wang, K. L., and Brown, K. W., "Free Electron Density and Transit Time in a Finite Superlattice," J. of Appl. Phys., 59(8), 2968 April (1986). (ONR)

Jogai, B., Wang, K. L., and Brown, K. W., "Frequency and Power Limit of Quantum Well Oscillators," Appl. Phys. Lett. 48(15), 1003 (1986). (ONR)

Sadwick, L. and Wang, K. L., "A Treatise on the Capacitance-Voltage Relation of HEMFET's", Transaction on Electronic Devices, ED-33(5), 651, (1986) (ONR, NSF)

Jogai B. and Wang, K. L., "High Frequency Amplification in Quantum Well Oscillators", in Superlattices and Microstructures, Vol.2, No.3, (1986). (ONR)

Xie, Y. H., R. People, J. C. Bean, and K. W. Wecht, "Power Loss by Two-Dimensional Holes in Coherently Strained Ge<sub>x</sub>Si<sub>1-x</sub>/Si Heterostructures: Evidence for Weak Screening.", Appl. Phys. Lett. 49, 283 (1986). (ONR)

Yuh, P. F. and Wang, K. L., "One Dimensional Transport in QWW-HEMT", Appl. Phys. Lett., 49(25), 1738, December (1986). (ONR, SRC)

Chung, S. K. and Wang, K. L., "Interface States of Modulation-Doped AlGaAs/GaAs Heterostructure", IEEE Transactions on Electron Devices, ED-34(2), 149 February (1987). (ONR, NSF)

de Frésart, E., Wang, K. L., and Rhee, S. S., "Auger Spectrometry and Scanning Electron Microscopy Study of the Interaction of B<sub>2</sub>O<sub>3</sub> with Silicon Surface," to appear in J. of Vac. Sci. & Tech., (1987). (ONR, SRC, ARO)

Jogai, B., and Wang, K. L., "Interband Optical Transitions in GaAs/GaAlAs Superlattices in an Applied Electric Field," Phys. Rev. B., 35(2) 653 January (1987). (ONR)

Jogai, B., Wang, K. L. and J. Schulman, "Intraband Optical Transitions in Superlattices.", to be submitted to Phys. Rev. B15., (1987). (ONR)

Yuh, P., and Wang, K. L., "A Novel Infrared Band-Aligned Superlattice (BAS) Laser", Appl. Phys. Lett., 51, 1404 (1987). (ONR, ARO, SRC)

E. de Fresart, K. L. Wang, S. S. Rhee, E. F. Gorey and W. M. Arienzo, "Evaluation of Boron-Doped Si Epilayers Grown by MBE", submitted to Journal of Vacuum Science and Technology (1987). (ONR, SRC, ARO)

Yuh, P. and Wang, K. L., "Intersubband Auger Recombination in a superlattice", to appear in Physical Review B, (1987). (ONR, ARO)

Jogai, B., and Wang, K. L., "Sensitivity of the Absorption Edge to the Applied Electric Fields in GaAs-GaAlAs Superlattices", to appear in Phys. Rev. Lett., (1987). (ONR, ARO)

Wang, K. L., "Elemental and Compound Semiconductor Devices Today and Beyond: Influence of Advanced Epitaxial Processes", SPIE's Proceedings Vol. 797, pp.2-12, (1987). (ONR, ARO, SRC)

Kang, T. W., Huang, C. F., Karunasiri, R. P. G., Park, J. S., and Wang, K. L., "Rheed Observation of MBE-Grown  $\text{GeSi}_{1-x}$  on Si(111)", to appear in J. of Vac. Sci. & Tech. B, (1987). (ONR, ARO, SRC)

#### CONTRIBUTIONS TO MEETINGS AND CONFERENCES

Jogai, B. and Wang, K. L., "Tunneling Current of Finite Superlattices with Various Well-Widths and Barrier Heights", March Meeting of the American Physical Society, March 25-29, 1985, Baltimore. (ONR)

Jogai, B. and Wang, K. L. "Light Induced Current in a GaAs/GaAlAs Superlattice", American Physical Society Meeting, Las Vegas, March 31 - April 4, (1986). (ONR)

Wang, K. L., "Silicon Molecular Beam Epitaxy", The Aerospace Corporation Special Conference on Electronic Materials, Los Angeles, October 1-2, (1986). (ONR, SRC, ARO)

Xie, Y. H., People, R., Bean, J. C., and Wecht, K., "Investigation on Energy Loss Mechanisms in MBE-Grown GeSi/Si heterostructure Using Shubnikov-de Haas Effect", the Seventh Molecular Beam Epitaxy Workshop, Massachusetts Institute of Technology, October 20-22, (1986). (ONR)

Lucas, A, de Fresart, E., Wang, K. L., Ostrom, R. and Allen, F. G., "Polariton Structure of Multilayered Semiconducting Materials, Proc. of the 18th Int'l. Conf. of Physics of Semiconductors, Stockholm, (1986). (ONR)

Huang, C. F., Karunasiri, R. P. G., Wang, K. L. and Kang, T. W. "Reflection High-Energy Electron Diffraction Observation of Substrate Cleaning During Silicon Molecular Beam Epitaxy", 2nd International Symposium on Silicon Molecular Beam Epitaxy, Hawaii, October 18-23, (1987). (ONR, SRC, ARO)

Wang, K. L., "Elemental and Compound Semiconductor Devices Today and Beyond: Influence of Advanced Epitaxial Processes", SPIE's Advances in Semiconductors and Semiconductor Structures", Bay Point, Florida, March 22-27, (1987). (Keynote Address) (ONR, ARO, SRC)

Jogai, B. and Wang, K. L., "Electroabsorption in GaAs- GaAl As Superlattices," American Physical Society, March Meeting, New York, March 16-20, (1987). (ONR)

Chern, C. H., Kao, Y. C., Neih, C. W., Jamieson, D., Bai, G., Wu, B. J., Mii, Y. J., Wang, K. L., and Nicolet, M-A. "MBE Growth of  $\text{GeSi}_{1-x}$  on Porous Silicon", 2nd International Symposium on Silicon Molecular Beam Epitaxy, Honolulu, Hawaii, October 18-23, 1987. (ONR, SRC)

Rhee, S. S., and Wang, K. L., "Ultraviolet Laser Assisted Silicon Molecular Beam Epitaxy Growth", 2nd International Symposium on Silicon Molecular Beam Epitaxy, Honolulu, Hawaii, October 18-23, 1987. (ONR, SRC)

Huang, C. F., Karunasiri, R. P. G., Park, J. S., Wang, K. L., and, Kang, T. W., "Surface Reconstruction of  $\text{Ge}_x\text{Si}_{1-x}$  on Si(111)", MRS Fall Meeting, Boston, 1987. (ONR, SRC)

Chang, S. J., Kallel, M. A., and Wang, K. L., "Strain Distribution of MBE Grown  $\text{Ge}_x\text{Si}_{1-x}$ /Si Layers by Raman Scattering", submitted to SPIE meeting, Spring 1988. (ONR)

5. APPENDICES

# Free-electron density and transit time in a finite superlattice

B. Jogai and K. L. Wang

*Devices Research Laboratory, Electrical Engineering Department, University of California at Los Angeles, Los Angeles, California 90024*

K. W. Brown

*Sensor Physics Section, Chemistry and Physics Laboratory, The Aerospace Corporation, El Segundo, California 90245*

(Received 11 November 1985, accepted for publication 2 January 1986)

In this paper we have calculated the free-electron density in a finite superlattice. Resonant tunneling causes a buildup of particle density in the well regions, giving rise to an accumulation of electrons in those regions. Using our results, we have estimated the change in barrier heights and well depths caused by the electrostatic force. A negligible change is found for a double-well structure having well widths of 40 Å and barrier widths of 20 Å. Our approach could be extended to calculate the tunneling current self-consistently. Additionally we have used a time-dependent solution of Schrodinger's equation to estimate the trapping time of the electrons due to the resonant effect. The results show that the probability density oscillates several times between the two wells, leaking out gradually at each step. After about  $2.4 \times 10^{-13}$  s, most of the waves centered about the resonant energies have been transmitted.

Copy available to DTIC does not permit fully legible reproduction

## INTRODUCTION

Interest in the finite superlattice, consisting of only a few layers, has been renewed due to the recent quality of thin films grown by molecular-beam epitaxy (MBE). Such a structure has potential device applications since the resonant tunneling phenomenon can lead to negative resistance. This effect had been predicted by Tsu and Esaki,<sup>1</sup> and subsequently verified by Chang *et al.*<sup>2</sup> Lately, there have been reports on measurements done on MBE-grown samples.<sup>3,4</sup> The results have included measurements of the current-voltage curve of a double-barrier device. In each case, the calculated tunneling current does not agree with the measured value for reasons that have not yet been clarified. In particular, the large peak-to-valley ratio predicted has not been realized experimentally. Discrepancies are to be expected, however, as the model is very simple. As an example, in the early calculation of the current, the conduction-band edge was modeled in a staircase approximation to account for the applied voltage. Semianalytic expressions were then obtained for the current. A numerical approach<sup>5</sup> has involved a more realistic treatment of the band edge, but the results are still not close to experiment.

In attempts to refine the model, it has been suggested that the well regions act as dynamic traps for the tunneling electron.<sup>6</sup> The presence of the electron in the well for some time is therefore expected to modify the potential. Deviation from linearity may occur. As a further refinement to the model, the tunneling current could be calculated self-consistently, taking into account the change in potential caused by the trapped electrons. We outline a way this can be done by calculating the free-electron density in the barrier and well regions, as a result of the accumulation of particle density in the well regions. Solution of Poisson's equation yields the modified potential. Such information can then be used to recalculate the electron density. Also presented is a time-dependent solution of Schrodinger's equation for a double-well triple-barrier structure. Multiple reflections of the elec-

tron wave packet are seen to increase the tunneling time by an order of magnitude over the classical limit.

## METHOD

Figure 1 shows the conduction-band edge of the structure that has been simulated. The free-electron density has been found by first obtaining the one-electron wave function. In the outermost GaAs layers, the wave functions are shown in Fig. 1, in which  $k_0^2 = 2m_{GaAs}^*(E - E_0)/\hbar^2$ ,  $k_1^2 = 2m_{GaAs}^*(E + eV_0 - E_0)/\hbar^2$ ,  $k_0^2 = 2m_{GaAs}^*E/\hbar^2$ .  $E_0$  is the energy in the GaAs regions corresponding to motion parallel to the interface plane.  $E$  is the total energy, and  $V_0$  is the applied voltage. The wave function for the barrier layers is given by

$$\Psi_k = [a \text{Ai}(-t_k) + b \text{Bi}(-t_k)] \exp(ik_0 \cdot \rho), \quad (1)$$

$$t_k = x_0^{-1} \gamma^{-1/2} [(E - eV_0 - \gamma E)/eF + z] \quad (2)$$

Here  $\text{Ai}$  and  $\text{Bi}$  are the Airy functions,  $F$  is the magnitude of the electric field,  $\gamma$  is the ratio of the effective mass in GaAs to that in  $\text{Ga}_{1-x}\text{Al}_x\text{As}$ ,  $x_0$  is a characteristic length given by  $x_0 = (2m_{GaAs}^*eF/\hbar^2)^{-1/2}$ , and  $V_0$  is the barrier height. For the well regions the wave function is given by



FIG. 1. Conduction-band edge of a multilayered GaAs-Ga<sub>1-x</sub>Al<sub>x</sub>As structure for an applied voltage  $V_0$ . The outermost GaAs layers are assumed to be heavily doped and semi-infinite in extent, so that the electric field in those regions can be assumed to be small, enabling the use of plane wave solutions. The rest of the structure is assumed to be intrinsic so that the electric field is taken to be a constant and in the negative  $z$  direction.  $V_0$  is the common barrier height.

# Frequency and power limit of quantum well oscillators

B. Jogai and K. L. Wang

Device Research Laboratory, Electrical Engineering Department, University of California, Los Angeles, Los Angeles, California 90024

K. W. Brown

Sensor Physics Section, Chemistry and Physics Laboratory, The Aerospace Corporation, El Segundo, California 90245

(Received 30 December 1985; accepted for publication 17 February 1986)

The maximum frequency at which amplification can be obtained from quantum well oscillators is discussed. Intrinsically, the frequency limit for having negative differential resistance (NDR) can be very high, of the order of the inverse of the electron transit time. Owing to the large capacitance of the well and barrier regions, the actual frequency limit at which amplification occurs may be lower than the intrinsic limit because of the capacitance charging time. We have estimated the frequency limit of NDR by considering the electron transit time and have calculated the maximum oscillation frequency from an equivalent circuit model. We have also obtained an expression for the high-frequency power output as a function of frequency, based on a transmission line model.

Negative differential resistance in quantum well devices is of considerable interest since the fast electron transport expected in such devices can result in high-frequency amplification. Tsu and Esaki<sup>1</sup> had predicted NDR in a finite superlattice as a consequence of resonant tunneling. The first experimental results were obtained by Chang *et al.*<sup>2</sup> Due to high input impedance, high-frequency oscillations were not observed in the early samples. Furthermore, the peak to valley ratio of the current was much too small to produce any workable power. Recent measurements on samples grown by molecular beam epitaxy<sup>3,4</sup> have shown promising results. Sollner *et al.*<sup>3,4</sup> have obtained a peak to valley ratio of 6:1,<sup>6</sup> and have also demonstrated mixing and detection at 138 GHz, 761 GHz, and 2.5 THz; these results suggest NDR up to 2.5 THz. In addition, they have used a coaxial resonant cavity to obtain oscillations at 18 GHz. If the electron transit time is the limiting factor for maximum oscillation frequency, an upper limit of about 1 THz seems possible. However, so far there has been no reported oscillation frequency in excess of 18 GHz.

In this letter, we discuss the maximum frequency at which NDR is possible as well as the maximum frequency at which a signal can be amplified by the quantum well device. In particular, we calculate the maximum frequency at which amplification is obtainable within a simple circuit model. We show that the circuit parameters which model the parasitic effects such as device capacitance and series resistance can have serious limitation on the maximum frequency of oscillation.

Previously Ricco and Azbel<sup>7</sup> have discussed the time development of resonant tunneling in a double barrier device, and have shown that an important quantity in determining frequency behavior is a time constant  $\tau$ , which is the time required for the probability density to build up in the well when a voltage is applied. Once this amount of time has elapsed, resonant tunneling is fully established. The frequency limit of NDR is expected to be set by the inverse of  $\tau$ . Luryi<sup>8</sup> has related the frequency limit of oscillation to the reciprocal of the charging time of a capacitor represented by

the first barrier layer; the second barrier is ignored in the estimate of the charging time. The charging current is assumed to be the single barrier tunneling current. A time constant of about 40 ps for the device of Refs. 3 and 4 is then obtained using the capacitance and positive resistance of the single barrier. In attempting to explain the higher observed detection frequencies,<sup>3</sup> Luryi proposed a new model in which the negative resistance is effected by the reduction in density of occupied emitter states allowed for tunneling with increasing applied voltage: when the quasibound level drops below the conduction-band edge of the emitter, there are no occupied emitter states consonant with energy and momentum conservation for tunneling. This effect as pointed out by Luryi, is of course, a generic feature to tunneling from a three-dimensional to a two-dimensional system of states. We note that this situation bears some resemblance to tunneling in a tunnel diode. Although the foregoing model for the existence of NDR is possible, it is not clear to us, however, that Sollner's detection of NDR at 2.5 THz depends upon the origin of the NDR.

An alternative explanation of the oscillation frequency and high-frequency detection may be possible and perhaps more appropriate. We are proposing an equivalent circuit model, based on which the oscillation frequency can be estimated from the magnitude of the NDR. The latter may be extracted from theoretical or experimental current-voltage curves if available. The results are independent of whether the NDR originates from the density of states or from the Fabry-Perot effect.

In quantum well devices where the NDR is accounted for by the Fabry-Perot mechanism, the speed at which the electron wave packet traverses the total structure is expected to govern the maximum frequency of amplification. Under ideal conditions, this maximum frequency should be close to the limit enforced by the transit time, since beyond this limit the NDR is annihilated, i.e., the negative conductance goes to zero. Recently, Barker<sup>9</sup> has calculated the tunneling time through a double-barrier device by solving Wigner's equation. A semiclassical formulation allows the effect of colli-

# A Treatise on the Capacitance-Voltage Relation of High Electron Mobility Transistors

LAURENCE P. SADWICK, STUDENT MEMBER, IEEE, AND K. L. WANG, SENIOR MEMBER, IEEE

**Abstract**—A new model for the capacitance-voltage relation of a HEMT is presented. The model uses three physically motivated capacitive terms in series. The  $C(V)$  expressions are derived using the quantum mechanical triangular potential well model and the two-dimensional electron-gas charge-control model. These expressions provide further physical insight into the AlGaAs heterosystem. The results obtained should be readily applicable to such techniques as DLTS and other  $C(V)$  interface measurement methods. The equations derived will also serve as a basis for analytical and circuit modeling of HEMT structures.

## NOMENCLATURE

$C$	Capacitance per unit area ( $F/cm^2$ ).
$D$	Density of states ( $cm^{-2} \cdot C^{-1} \cdot V$ ).
$d_2$	Total width of AlGaAs epilayer (cm).
$E_C$	Conduction band energy (eV).
$E_F$	Fermi energy (eV).
$E_n$	subband energy (eV).
$F_i$	Electric field at interface ( $V/cm$ ).
$N_B$	Background doping level in GaAs ( $cm^{-3}$ ).
$N_{dep}$	Effective depletion surface layer charge in GaAs ( $cm^{-2}$ ).
$n_s$	Two-dimensional electron sheet concentration ( $cm^{-2}$ ).
$S$	Spacer layer thickness (cm).
$V_{FE}$	Voltage difference between conduction band and Fermi level in AlGaAs (V).
$V_G$	Applied gate voltage (V).
$V_{G_0}$	Applied gate voltage which maintains equilibrium conditions at heterointerface (threshold voltage for charge control [7]) (V).
$V_{OFF}$	Annihilation voltage that extinguishes $n_s$ (V).
$V_2$	Depletion voltage across the doped AlGaAs layer (V).
$V_{20}$	Equilibrium band bending on the AlGaAs side of the heterointerface (V).
$W$	Width of undoped GaAs epilayer (cm).
$Z_n$	Average distance of electrons in the $n$ th subband from the interface (cm).
$\Delta E_C$	AlGaAs/GaAs conduction band discontinuity (V).
$\phi_B$	Schottky-barrier height of metal-AlGaAs system (V).

Manuscript received October 1, 1985; revised November 2, 1985. This work was supported in part by the National Science Foundation and by the Office of Naval Research.

The authors are with the Device Research Laboratory, Electrical Engineering Department, University of California, Los Angeles, CA 90024.  
IEEE Log Number 86-2722.

## I. INTRODUCTION

RECENTLY, there has been a great deal of interest and activity in the area of HEMT (also known as MODFET, TEGFET, and SDHT) and other similar two-dimensional gas structures for the design of high-speed and high-frequency devices [1]–[3]. The two-dimensional nature of the electron gas sheet arises from the transfer of mobile charges from the larger bandgap material to the smaller one at the heterointerface due to the band discontinuity. Usually the device is operated at low temperatures (e.g., 77 K) to reduce the electron-phonon scattering, which degrades the mobility. At 77 K, the remaining dominant scattering mechanism is impurity scattering. In an AlGaAs/GaAs heterojunction structure, the impurity scattering for the transferred two-dimensional electron gas is reduced due to the separation of the parent donor impurity atoms in the  $Al_{1-x}Ga_xAs$  from the undoped GaAs. To reduce further impurity scattering, a spacer layer of undoped AlGaAs is placed between the GaAs and the heavily doped AlGaAs [4]. Several studies have been done to determine the optimum thickness of the spacer layer [5], [6].

## II. THE MODEL

The two-dimensional electron gas is assumed to lie in a quantum mechanical triangular potential well that arises from the coupling of Schrodinger's equation and Poisson's equation through the potential term given by the linear function  $V(x) = -Fx$ , where  $F$ , the electric field, is assumed constant. Referring to Fig. 1, one has the following well-accepted expression for the two-dimensional electron sheet concentration [7]:

$$n_s = D \left\{ \ln \left( 1 + \exp \frac{(E_t - E_0)}{kT} \right) + \ln \left( 1 + \exp \frac{(E_F - E_1)}{kT} \right) \right\} \quad (1)$$

where  $D$  is the density of states in units of reciprocal square centimeters per coulombs times volts and  $E_0$  and  $E_1$  are the lowest energy of the zeroth and first subbands, respectively, whose energy is given approximately by [8], [10]

$$E_n = \left( \frac{\hbar^2}{2m} \right)^{1/3} \left( \frac{3}{2} \pi q F \right)^{2/3} \left( n + \frac{3}{4} \right)^{2/3} \quad (1a)$$

## HIGH FREQUENCY AMPLIFICATION IN QUANTUM WELL OSCILLATORS

B. Jogai and K. L. Wang  
 Device Research Laboratory  
 University of California at Los Angeles  
 Los Angeles, California 90024  
 K. W. Brown  
 The Aerospace Corporation  
 El Segundo, California 90245

Received 3 March 1986

We have calculated the frequency limit of negative differential resistance and a.c. amplification of quantum well oscillators. From the time development of resonant tunneling, negative resistance is expected to occur at very high frequencies. However, the large device impedance results in a resistive cut-off frequency that is several orders of magnitude below that predicted from transit time considerations. This cut-off frequency is estimated from an equivalent circuit model, and the power of an oscillator as a function of frequency and negative resistance is found from a transmission line model.

### 1. Introduction

Quantum well structures are of considerable interest as a.c. amplifiers and active power sources since the interference phenomenon (i.e. resonant tunneling) in these devices can give rise to Negative Differential Resistance (NDR). A typical device size is of the order of a few tens of nanometers. With collisions virtually eliminated at low temperatures, very fast electron transport is anticipated, promising amplification at frequencies beyond that currently obtainable from conventional devices such as IMPATT and Tunnel diodes.

The first such device was a double-barrier GaAs/GaAlAs structure grown by Chang et al.<sup>1</sup> Although negative resistance was clearly demonstrated, the peak to valley ratio of the current was not large enough to produce any significant output power. Recent results on samples grown by molecular beam epitaxy<sup>2-4</sup> have yielded more encouraging results. Sakaki<sup>3</sup> has obtained a peak to valley ratio of 10:1.

Earlier, Sollner et al.<sup>2,4</sup> had obtained a peak to valley ratio of 6:1 and had demonstrated mixing and detection at 138 GHz, 761 GHz, and 2.5 THz, these results appear to suggest NDR up to 2.5 THz. Sollner et al.<sup>4</sup> also obtained oscillations at 18 GHz using a coaxial resonator. This value is much lower than the limit of a few THz anticipated from the electron transit time. So far, however, there has been no reported oscillation frequency in excess of 18 GHz.

In this paper we explore the high frequency behaviour of the quantum well device. In

section II we consider the frequency limit of NDR based on the time development of resonant tunneling. On the basis of transit time considerations, an intrinsically high limit is obtainable. In section III an equivalent circuit model is used to find the maximum oscillation frequency. The physical properties of the device are represented phenomenologically by the circuit parameters which can be extracted from experimental or theoretical current-voltage curves. We show that the circuit elements can seriously affect the oscillation frequency limit. Finally, in section IV we estimate the power-frequency behaviour, assuming that the device is operated in a coaxial resonant cavity.

### II. Frequency Limit of Negative Differential Resistance

Previously the time dependence of resonant tunneling has been discussed by Ricco and Azbel<sup>5</sup> for a double-barrier device. Both transient and steady state phenomena have been considered. As they have pointed out, a formerly overlooked factor in measuring the current-voltage response is the charge build-up time in the well region. The well behaves as a dynamic trap, causing electrons to spend some time there before finally leaking out. Resonant tunneling is established once the outgoing flux equals the incoming flux. In addition to the trapping and build-up times, there is a feedback mechanism which is further expected to delay the onset of resonance: the trapping process causes an accumulation of charge which in turn modifies the potential energy. As shown by Ricco and Azbel, the build-up time is non-negligible. This property of resonance tunneling

# Power loss by two-dimensional holes in coherently strained $\text{Ge}_{0.2}\text{Si}_{0.8}/\text{Si}$ heterostructures: Evidence for weak screening

Y. H. Xie\*

Department of Electrical Engineering, University of California, Los Angeles, California 90024

R. People, J. C. Bean, and K. W. Wecht

AT&T Bell Laboratories, Murray Hill, New Jersey 07974

(Received 14 April 1986; accepted for publication 10 June 1986)

We have used the hot-carrier Shubnikov-de Haas effect to measure the power loss by hot two-dimensional holes in coherently strained  $\text{Ge}_{0.2}\text{Si}_{0.8}/\text{Si}$  heterostructures. The measured power loss versus carrier temperature data are best described by the two-dimensional formalism of P. J. Price [J. Appl. Phys. 53, 6864 (1982)] assuming weak screening. Excellent agreement with experiment is obtained only if scattering of the acoustic mode phonons by both the deformation potential and the piezoelectric coupling mechanisms are considered. We are therefore able to deduce a value for the piezoelectric constant for  $\text{Ge}_{0.2}\text{Si}_{0.8}$ , which is approximately 35% of that for InAs ( $e_{31}^2 \approx 0.22 \times 10^6$  dyne/cm<sup>2</sup>). In light of the fact that charge transfer effects are expected to be small in bulk (unstrained)  $\text{Ge}_x\text{Si}_{1-x}$ , the present observations are indicative of either a large strain induced change in ionicity or of scattering of acoustic phonons from ordered domains via the piezoelectric mechanism.

The subject of power loss by hot carriers in highly degenerate two-dimensional systems confined at semiconductor-semiconductor heterointerfaces has recently received much theoretical attention.<sup>1-3</sup> Measurements of the electron temperature and power loss by hot two-dimensional electrons in  $\text{GaAs}/\text{Al}_x\text{Ga}_{1-x}\text{As}$  heterostructures have been mainly confined to photoexcitation experiments.<sup>4-6</sup> Photoexcitation experiments have given a wealth of information on power loss and distribution functions for the case in which power loss occurs predominantly by emission of polar optic (LO) phonons. These results have also demonstrated the importance of screening of the electron-LO phonon interaction,<sup>7</sup> and have in general served to test existing two-dimensional (2D) theories for polar optic phonon mediated power loss.

Recently Bozler *et al.*<sup>8</sup> have obtained data on power loss as a function of carrier temperature due to electric field heating of 2D electrons in  $\text{GaAs}/\text{Al}_x\text{Ga}_{1-x}\text{As}$  multiple quantum wells at very low temperatures ( $50 \text{ mK} < T < 1 \text{ K}$ ). These data are indicative of either piezoelectric dominated power loss with strong screening of the electron-acoustic phonon interaction or of deformation potential dominated power loss with weak screening of the electron-acoustic phonon interaction, the appropriate mechanism remains indeterminate. Experiments on highly degenerate two-dimensional hole systems wherein power loss occurs predominantly by acoustic mode scattering with deformation potential and/or piezoelectric couplings are lacking, however.

In the present letter we present measurements of power loss due to electric field heating of a highly degenerate 2D hole gas in coherently strained  $\text{Ge}_{0.2}\text{Si}_{0.8}/\text{Si}$  heterostructures.<sup>9</sup> To the extent that the  $\text{Ge}_{0.2}\text{Si}_{0.8}$  alloy exhibits some degree of ordering,<sup>10</sup> this system retains the necessary attributes for the observation of a piezoelectric effect (i.e., dissimilar atoms along with a noncubic unit cell). When investigating contributions to the power loss one must therefore

consider the scattering of carriers by acoustic mode phonons due to the deformation potential as well as the piezoelectric interaction. Further, since the calculated temperature dependence of the power loss by these mechanisms<sup>3</sup> yields very dissimilar (power law) results when screening effects are present or absent, we are able to quantify the extent to which screening of the hole-acoustic phonon interaction is important in the present system.

Samples were grown using Si molecular beam epitaxy in a  $\text{Si}/\text{Ge}_x\text{Si}_{1-x}/\text{Si}$  single wide quantum well ( $L_w \equiv L_{\text{min}}, = 500 \text{ \AA}$ ) configuration. The Si layers were selectively doped  $p$  type ( $\sim 10^{18} \text{ cm}^{-3}$ ) with boron whereas the  $\text{Ge}_x\text{Si}_{1-x}$  alloy (having  $x = 0.2$ ) was not intentionally doped. A dopant setback of  $250 \text{ \AA}$  was present in the Si layers adjacent to the  $\text{Ge}_x\text{Si}_{1-x}$ . Low electric field Shubnikov-de Haas data indicated the population of a single subband, having a sheet charge density  $n_{2D} \approx 5 \times 10^{11} \text{ cm}^{-2}$ , ( $E_F - E_0) \approx 5 \text{ meV}$ , carrier effective mass  $m^* \approx 0.27m_0$ , and Hall mobility  $\mu_h \sim 3300 \text{ cm}^2 \text{ V}^{-1} \text{ s}^{-1}$ . For the given sheet charge density, a  $500\text{-\AA}$  well is expected to be transformed by the space-charge field to two single interface heterolayers, resulting a greater level spacing, which is consistent with the occupation of a single subband. Measurements were performed under perpendicular magnetic fields up to  $100 \text{ kG}$  at temperatures ranging from  $1.75$  to  $4.5 \text{ K}$ . The electric field strength was deduced from the measured longitudinal voltage drop, taking into account the device geometry. No detectable change in mobility occurred over the aforementioned temperature range and for electric field strengths between  $1.8 \text{ mV/cm}$  and  $2.5 \text{ V/cm}$ .

The relation between carrier temperature and electric field was obtained using the hot-carrier Shubnikov-de Haas (SdH) effect.<sup>11</sup> In his procedure, the extreme sensitivity of the amplitude of the quantum oscillations is used as a measure of temperature. One first measures the longitudinal magnetoresistance ( $\rho_{xx}$ ) over a range of lattice temperatures  $T$ , for a fixed, very low value of the electric field. Typical data are shown in Fig. 1(a), for  $\xi = 1.8 \text{ mV/cm}$  and  $1.75$

\*AT&T Bell Laboratories scholar.

# One-dimensional transport in quantum well wire-high electron mobility transistor

Perng-fei Yuh and K. L. Wang

Device Research Laboratory, Department of Electrical Engineering, University of California, Los Angeles, California 90024

(Received 25 July 1986, accepted for publication 31 October 1986)

A novel one-dimensional electron gas field-effect transistor (FET) is proposed with the advantages of higher electron mobility and higher carrier concentration than conventional two-dimensional electron gas FET. The FET structure, device operation, and the low-field mobility of impurity scattering, which takes the screening effect into account, are discussed.

Molecular beam epitaxy technology has made ultrathin heterostructures possible. One recent application using those heterostructures is the high electron mobility transistor (HEMT). Its basic idea is to separate the two-dimensional (2D) electron gas in the heterolayer to reduce Coulombic scattering from their mother donors in the heavily doped wide band-gap material, thus yielding high mobility, especially at low temperature.<sup>1</sup> Although the saturation velocity of 2D gas is about equal to that in the bulk GaAs, the high low-field mobility should still improve the device performance due to the field distribution in field-effect transistor (FET).<sup>2</sup> By further confining the dimensions, i.e., reducing from two dimensions to one dimension, quantum well wires (QWW's) are suggested to have the advantage of high mobility.<sup>3</sup> Several possible device structures using QWW's have been proposed.<sup>4</sup> A primitive QWW has been fabricated.<sup>5</sup> In this letter, we analyze the FET operation and transport properties of a QWW HEMT. It shows that the low-field mobilities due to impurity scattering with and without screening are much higher than that in HEMT.

The basic structure is shown in Fig. 1(a), which depicts one side of the *V*-groove or *U*-groove structure similar to that of Sakaki.<sup>6</sup> Our structure uses QWW with carriers separated from the donors by a spacer similar to the 2D HEMT. The complete view of an FET is shown in Fig. 1(b). Quantum well dots may be obtained in this structure if the gate strip can be made very narrow.<sup>7</sup> For a single channel, the energy-band diagram is shown in Fig. 1(c). The concentration of one-dimensional carriers in the channel is controlled by the gate voltage. In the *x* direction, electrons are confined in a triangle well (an approximated form). In the *y* direction, it is a square well. Electron motion is restricted only to the *z* direction, thus a one-dimensional electron gas is formed.

For a single channel, one may plot the ionized impurity charge, 1D electron, and the electric field distribution as in Fig. 2. The 1D electrons may be treated as if they come from the depleted *n*-AlGaAs layer. Since the fringe effect is significant, the concentration of 1D gas is usually higher than the 2D gas in HEMT, i.e.,  $n_{1D} > n_{2D} \times L_1$ . From Gauss's law, the 1D carrier concentration (C/cm) is  $qn_{1D}(z) = \epsilon_1(L_1\bar{E}_x + 2W_1\bar{E}_y)$ , where  $W_1$  is the depletion width of undoped GaAs,  $L_1$  is the thickness of GaAs layer, and  $\epsilon_1$  is the dielectric constant of GaAs. Here, we assume that the depletion charge of undoped GaAs or AlGaAs and the interface charge at the AlGaAs/GaAs heterolayers can be neglected; for otherwise the 1D carrier concentration may be-

come lower.  $\bar{E}_x(W_1, y) = 0$  and  $\bar{E}_x, \bar{E}_y$  are the suitable average values.  $\bar{E}_x$  has been solved for HEMT,<sup>2</sup> while  $\bar{E}_y$  should take into consideration the fringe effects. When all channels are very close,  $\bar{E}_y$  may be approximated as  $\epsilon_1 2W_1\bar{E}_y \approx aL_2\epsilon_1\bar{E}_x$ , where  $a < 1$  is a factor to take into account the 2D fringe effects of the electric field and  $L_2$  is the layer thickness of AlGaAs. Following the same derivation of HEMT,<sup>6</sup> one may easily obtain the current-voltage (*I*-*V*) relation in the linear region as

$$I_D = (1/L_1) [N_c \mu \epsilon_2 / (d_2 + \Delta)] (L_1 + aL_2) \times [(V_G - V_T)V_D - \frac{1}{2}V_D^2], \quad (1)$$

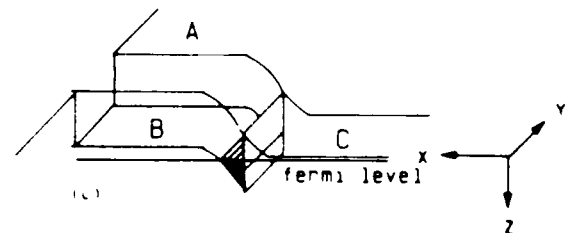
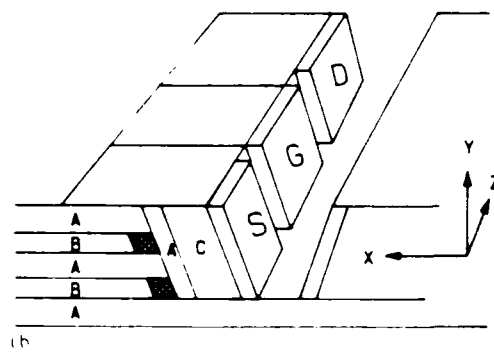
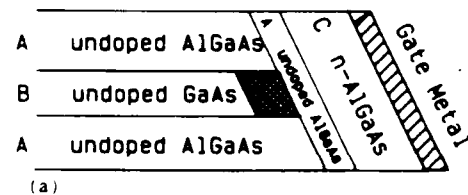


FIG. 1. Structure and band diagram of the QWW HEMT. (a) Single channel quantum well wire HEMT. One-dimensional electron gas is confined in the shaded area. (b) Complete view of an FET. Current transport is in the *x* direction. The 1D carriers in the channel are controlled by the gate voltage. (c) Energy-band diagram for one channel of the QWW HEMT, a triangle potential well along the *x* direction and a square potential well along the *z* direction.

# Interface States of Modulation-Doped AlGaAs/GaAs Heterostructures

SANG-KOO CHUNG, Y. WU, K. L. WANG, N. H. SHENG, C. P. LEE, AND D. L. MILLER

**Abstract**—We have used the admittance spectroscopy to investigate interface states associated with heterojunction of modulation-doped AlGaAs/GaAs FET's. Anomalous frequency dispersion of the capacitance was observed. The results of the measurements were interpreted in terms of an equivalent circuit containing a series resistance of the two-dimensional electron gas in the ungated region between the gate and the source and drain electrodes. The maximum density of the interface states was found to be  $1.3 \times 10^{12} \text{ cm}^{-2} \cdot \text{eV}^{-1}$  around 0.13 eV below the  $E_c$  edge of GaAs.

## I. INTRODUCTION

RECENTLY, modulation-doped FET's or high electron mobility transistors (HEMT's) have been actively studied for high-speed applications [1]–[4]. The high mobility of the two-dimensional electron gas formed in the interface of an AlGaAs/GaAs heterojunction results from the reduced Coulomb scattering in the channel by spatially separating the electrons from their parent donor impurity ions with a heterostructure. The interfacial properties of the epitaxial GaAs and AlGaAs are therefore of fundamental importance to the operation of the devices.

In this paper we present the results of admittance measurements on HEMT's and introduce an equivalent circuit of the AlGaAs/GaAs heterojunction capacitor, which allows a realistic characterization of the interface states of the heterojunction.

The anomalous frequency dispersion of the admittance was observed and attributed to a high density of fast interface states of the heterojunction and to the series resistance of the two-dimensional electron gas in the ungated region between the gate and the source and the drain electrodes.

## II. ADMITTANCE MEASUREMENTS

The structure and the contacts of a AlGaAs/GaAs HEMT grown by the MBE technique are shown in Fig.

Manuscript received August 31, 1984; revised August 30, 1985. This work was supported in part by the Semiconductor Research Corporation and the Office of Naval Research.

S. K. Chung is on leave with the Device Research Laboratory, Electrical Engineering Department, University of California, Los Angeles, CA 90024. He is with Ajou University, Suwon, Korea.

Y. Wu is on leave with the Device Research Laboratory, Electrical Engineering Department, University of California, Los Angeles, CA 90024. He is with the Shanghai Institute of Technical Physics, Shanghai, China.

K. L. Wang is with the Device Research Laboratory, Electrical Engineering Department, University of California, Los Angeles, CA 90024.

N. H. Shen, C. P. Lee, and D. L. Miller are with Rockwell International, Thousand Oaks, CA 91360.

IEEE Log Number 8611368

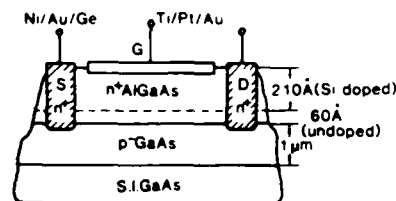


Fig. 1. Structure and contacts of high electron mobility AlGaAs/GaAs FET used in admittance measurement

1. The samples used in this study consist of a 1- $\mu\text{m}$ -thick undoped p-type GaAs epitaxial layer grown on a semi-insulating GaAs substrate, followed by 60- $\text{\AA}$  undoped  $\text{Al}_{0.3}\text{Ga}_{0.7}\text{As}$ , and then a 210- $\text{\AA}$   $n^+$ - $\text{Al}_{0.3}\text{Ga}_{0.7}\text{As}$  layer heavily doped with Si to  $10^{18} \text{ cm}^{-3}$ . This structure is identical to the modulation-doped heterostructure. A Au/Ge/Ni ohmic contact was provided to the two-dimensional electron gas while a Ti/Pt/Au contact forms metal Schottky contact with a gate area of  $9 \times 10^{-4} \text{ cm}^2$ .

With a Schottky gate on the AlGaAs layer, there exists a certain depletion region under the gate. If the AlGaAs layer is thin enough that the gate depletion and junction depletion regions overlap [5], the HEMT may be treated like a MIS capacitor with the wide-energy-gap AlGaAs layer as an insulator. The characterization of this capacitor may be used to extract the interfacial properties of the heterojunction from admittance measurement.

Capacitance and conductance measurement were performed with help of a Hewlett-Packard multifrequency LCR meter, model 4275A. The RF signal amplitude was kept at 20 mV so that the small-signal condition prevails. The bias voltage was not allowed to exceed +0.2 V, to prevent forward current conduction. A positive bias is defined for a positive potential connected to the Schottky gate contact.

The measured  $C$ - $V$  and  $G$ - $V$  characteristics are shown in Fig. 2. The seemingly anomalous frequency dependence of the  $C$ - $V$  curves with capacitance decreasing with increasing frequency can be expected when a number of fast surface states play the dominant role. The conductance peaks show a strong dispersion with the peaks shifting to higher bias with increasing frequency. The presence of a peak in the  $G$ - $V$  curve is associated with the effective loss due to the interfacial traps [6]. However, a further increase of the conductance as the bias increases positively indicates other loss mechanisms. The peak, due

**AUGER SPECTROMETRY AND SCANNING ELECTRON MICROSCOPY STUDY  
OF THE INTERACTION OF  $B_2O_3$  WITH SILICON SURFACE.**

E. de Frésart, K.L. Wang and S.S. Rhee  
Device Research Laboratory  
Electrical Engineering Department  
University of California at Los Angeles  
Los Angeles, CA 90024

**ABSTRACT**

Interaction of monolayer  $B_2O_3$  with Si surface has been studied by Auger electron spectroscopy (AES) and scanning electron microscopy (SEM) as a function of the substrate temperature  $25^\circ\text{C} < T_s < 760^\circ\text{C}$ . For  $T_s < 500^\circ\text{C}$ ,  $B_2O_3$  adsorbs molecularly on the surface. No chemical reaction is observed between both components. For  $T_s > 500^\circ\text{C}$ ,  $SiO_2$  and B (or silicon boride compound) new phases are growing at the expense of  $B_2O_3$ .  $SiO_2$  is subsequently decomposed into SiO which desorbs for  $T_s > 600^\circ\text{C}$ . Reduction of  $B_2O_3$  and  $SiO_2$  are completely achieved at  $760^\circ\text{C}$ . At this temperature, SEM shows nucleation of spheroidal particles. We developed a model based on a theory of diffusion-controlled growth of spheroidal particles ( $SiO_2$ , B or silicon boride) from the decomposition of a supersaturated solution ( $B_2O_3$  saturated by Si). Atomic fractions data have been fitted to the Avrami's kinetics equation  $I \approx 1 - \exp[-K(2Dt)^n]$  with good agreement. Activation energy of the diffusion coefficient D has been calculated to be  $E_a = 0.87 \pm 0.2$  eV, assuming that the exponent  $n=1$ .

Interband optical transitions in GaAs-Ga<sub>1-x</sub>Al<sub>x</sub>As superlattices in an applied electric field

B. Jogai and K. L. Wang

*Device Research Laboratory, Department of Electrical Engineering, University of California at Los Angeles, Los Angeles, California 90024*

(Received 11 July 1986)

We have investigated the light absorption in a GaAs-Ga<sub>1-x</sub>Al<sub>x</sub>As superlattice in the presence of an applied electric field. Using Houston functions to represent the valence and conduction states we have calculated the transition rates between the valence and conduction subbands for different values of the field. Both the Franz-Keldysh shift and Franz-Keldysh oscillations emerge from the formalism. The absorption edge as a function of photon energy varies exponentially and has small oscillations superimposed on it. It is followed by a flat region characteristic of a two-dimensional electron gas. The use of Houston functions is justified by computing the tunneling probability between adjacent subbands and showing that it is negligibly small.

## 1. INTRODUCTION

Light absorption in superlattices and quantum wells in the presence of an electric field has been investigated in the recent literature for possible applications in electro-optics. Recent experiments have shown that the absorption coefficient is strongly affected by an applied electric field.<sup>1-4</sup> The modulation of the absorption coefficient has led to the proposal of a new class of switching devices<sup>5,6</sup> which can be operated by changing the field applied to the superlattice structure, thereby creating "on" and "off" transmission states for the light wave. In the superlattice case absorption can occur for photon energies both above and below the superlattice band gap. The latter is the usual Franz-Keldysh effect.<sup>7</sup> Unlike bulk material, the absorption edge is anticipated to be more sensitive to the field, a consequence of the lowering of the effective superlattice band gap. This effect originates from the polarization of the superlattice envelope function by the electric field and may be of the order of a few meV. For bulk material, on the other hand, the effect is small because the host Brillouin zones are not seriously distorted for fields below the avalanche breakdown. Switching can thus be effected using a superlattice for photon energies below the band gap since the electric field can be used to turn the transmission "on" and "off." The feasibility of switching with the band gap depends on the sensitivity of the absorption to the electric field. Assuming that the absorption coefficient can be adequately represented by a step function, the superlattice is useful for integral-optical devices where the light consists of the electrons moving in the field.

The purpose of this paper is to investigate the light absorption in GaAs-Ga<sub>1-x</sub>Al<sub>x</sub>As superlattices in the presence of an applied electric field. In Sec. II we study the theory of light absorption in superlattices in the presence of an electric field. In Sec. III we calculate the absorption coefficient for a superlattice with a band gap above the superlattice band gap. A comparison is made with the results of a superlattice with a band gap below the superlattice band gap. In Sec. IV we discuss the results for a quantum well (MQW) structure. In Sec. V we discuss the results for a superlattice structure.

wave-function overlaps have been worked out using suitable model potentials to represent the superlattice and MQW. In Ref. 8 the Ga<sub>1-x</sub>Al<sub>x</sub>As layers are considered sufficiently thick that the electrons and holes cannot tunnel between adjacent wells. In fact Miller *et al.*<sup>8</sup> considered the ideal case where the potential barrier is infinite. The electric field was incorporated by tilting the bottom of the well. The authors then computed the red shift and showed from their bound-state model the closeness between the Stark shift and the Franz-Keldysh effect. McIlroy<sup>9</sup> calculated the change in overlap between the electrons and holes in an MQW caused by an electric field, a prerequisite to understanding the electroabsorption phenomenon in these structures. McIlroy imposed an artificial boundary condition on the MQW by sandwiching it between semi-infinite barrier layers having constant potentials. Since both approaches are essentially bound-state models, they yield absorption coefficients that consist of a superposition of step functions and are characterized by abrupt increases as the photon energy is increased. Such results are characteristic of the two-dimensional bound-state problem and are a consequence of the electron being unable to tunnel out of the structure. When an electric field is applied, the function is simply shifted to the left. In the conventional terminology, this is due to the Stark lowering of the bound electron and hole states. But as pointed out in Refs. 8 and 9, once a field is applied, there are no true bound states. This is especially true for the superlattice and MQW where the barrier heights are small (typically around 0.25 eV). And since the particles now exist in the quasibound states for only a short time (e.g., 10<sup>-12</sup> s), the problem is essentially similar to the bulk (i.e., three-dimensional) and therefore a considerable smearing out of the steplike behavior is expected. Conventionally, the red shift with increasing field for continuum states is the Franz-Keldysh effect. For the superlattice and MQW the two effects are clearly related. However, in this paper we denote the red shift in our model as the Franz-Keldysh effect in keeping with the usual notation.

Our calculations differ from those of Refs. 8 and 9 in the important aspect of boundary conditions, we avoid the use of restrictive end conditions usually necessary for

Copy available to DTIC does not permit fully legible reproduction

# *Intraband Optical Transitions in Superlattices*

B. Jogai and K.L. Wang

*Device Research Laboratory, Department of Electrical Engineering, University of California, Los Angeles, California 90024*

J.N. Schulman

*Hughes Research Laboratories, Malibu, California 90265*

## **ABSTRACT**

Phononless intraband absorption in superlattices has been investigated theoretically. Using GaAs-Ga<sub>1-x</sub>Al<sub>x</sub>As as an example, the absorption coefficient for optical transitions between the conduction sub-bands has been calculated. Because of singularities in the joint density of states, the absorption is enhanced at the zone center and zone boundary of the mini-Brillouin zone. The results suggest the possibility of utilizing intraband absorption for long wavelength infra-red detection.

# Novel infrared band-aligned superlattice laser

Copy available to DTIC does not permit fully legible reproduction

Peng-fei Yuh and K. L. Wang

Device Research Laboratory, Department of Electrical Engineering, University of California, Los Angeles, California 90024

(Received 4 May 1987; accepted for publication 1 September 1987)

A novel infrared laser is proposed which uses the intersubband optical transition in a band-aligned superlattice. In this band-aligned superlattice laser, the miniband discontinuity within the conduction or valence band functions as a band offset in the heterojunction structure, and the population inversion is achieved by current injection as in the conventional heterojunction laser. It is more flexible than a heterojunction laser or a quantum well laser since one may tailor the bandwidth and band structures as well as the band gap of the minibands. Also indirect band-gap materials like Si and Ge can be used for lasing in the intersubband transitions. The intersubband optical transition is similar to an atomic two-level system which exhibits low threshold current, and a gain coefficient with weak temperature dependence and a narrow spectrum which is determined only by the line-shape function. These special features make the band-aligned superlattice laser competitive with and perhaps superior to the quantum well dot laser which is not presently feasible.

Recently advances in microstructure technology in semiconductors like molecular beam epitaxy (MBE) and electron beam lithography have made ultrathin and ultra-small novel structures possible. Among these, the electronic and optical properties of the quantum well and superlattice have been extensively studied because of their interesting physical phenomena and possible device applications.

The optical properties of the quantum well were first investigated by Dingle<sup>1</sup> in 1975. Since then the quantum well laser has received considerable attention because of its low threshold current and weak temperature dependence.<sup>2</sup> Although the intersubband transition in a quantum well has been considered for possible novel infrared detectors,<sup>3,4</sup> its application to lasers or light-emitting diodes has not been explored. Here the term "intersubband transition" is used to refer the subband-to-subband transition within the conduction or valence band. The advantages of intersubband transitions in a superlattice are that the miniband bandwidth as well as the band gap can be tuned by changing the barrier and well width and the barrier height. Because the transition frequency is in the infrared spectrum, quantum wells and superlattices can be substituted for the narrow band gap IV-VI or II-VI compounds in photonic applications. Also, indirect band-gap materials such as Si and Ge can be candidates for lasing in the intersubband transition frequencies in a quantum well or a superlattice since the intersubband transition is direct regardless of the host material.

A typical band structure of the proposed superlattice laser is shown in Fig. 1. There are three regions in this multiple superlattice. In region I, the superlattice well is thin, so that only one miniband is allowed. In region II, the superlattice well and barrier are specially designed such that two minibands are formed where the upper miniband is aligned to the miniband of the first region. In region III, two minibands are formed. However, only the lower miniband is aligned with the lower band of the second region. The upper band of the third region is above the upper band of the second to form a man-made band discontinuity in the subbands of the superlattice. These minibands are schematically

shown in Fig. 1 under an applied bias  $V_{bias}$ . Electrons are injected from the region I superlattice into the upper miniband of the region II superlattice, but are blocked at the boundary of the region III superlattice due to a miniband discontinuity there. The lower miniband of the region II superlattice is depleted by the current flowing out through the lower miniband of the region III superlattice. Region II now serves as the active region, while the other two regions behave like the *p* and *n* regions as in conventional heterojunction lasers. The region II superlattice may be replaced by a parabolic or V-shaped well in order to have the bands aligned to the neighboring superlattice. Since the miniband alignment and offset is introduced in the superlattices for efficient current injection, we call this new type of infrared laser the band-aligned superlattice laser (BAS laser). For example, a miniband separation of 0.124 eV will be a lasing frequency  $\approx 12400/0.124 \text{ \AA} = 10 \text{ \mu m}$  which is in the infrared range, within the transmission window of the atmosphere. The intersubband transitions in superlattices offer many options. A doped superlattice may be used as well as the compositional superlattice. In addition to the wide band-gap III-V compounds, indirect band-gap materials such as Si and SiGe may be used for lasing in the intersubband transitions. This implies that this BAS laser may be integrated monolithically on a silicon very large scale integrated chip. The operating frequency may be adjusted by tailoring the superlattice barrier

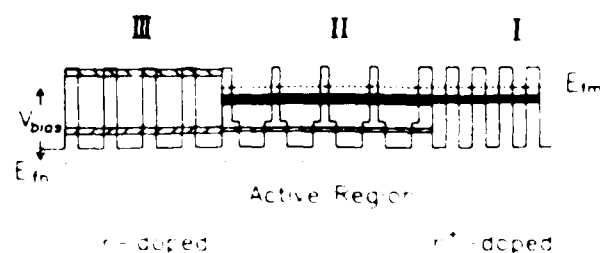


FIG. 1. Band aligned superlattice (BAS) laser using intersubband optical transition and miniband discontinuity. The superlattice in region II may be replaced by a parabolic or V-shaped well superlattice. The discontinuity II is between that in region I and region III.

EVALUATION OF BORON-DOPED SI EPILAYERS  
GROWN BY MOLECULAR BEAM EPITAXY

E. de Frésart\*, K.L. Wang and S.S. Rhee  
Device Research Laboratory, Electr. Eng. Dept.  
University of California at Los Angeles, CA 90024  
E.F. Gorey and W.N. Arienzo  
IBM, Thomas J. Watson Research Center  
Yorktown Heights, NY 10598

We present a detailed evaluation of boron-doped Si epilayers on both (100) and (111) orientations grown by Si molecular beam epitaxy, using boron oxide as a dopant source from an effusion cell.

Boron incorporation in the film is the result of  $B_2O_3$  decomposition by successive reactions with Si which form lower boron oxides and  $SiO_2$  phases, and by the subsequent removal of  $SiO_2$  under the SiO form. A theoretical model of the reaction kinetics is deduced from in-situ Auger experimental measurements.

Morphology and crystallinity of the epilayers were studied for different doping concentrations as a function of the growth temperature ( $400^\circ\text{C} < T < 900^\circ\text{C}$ ) using the defect etch technique and electron channeling. Three temperature regions are observed, revealing amorphous, polycrystalline and epitaxial growth when going from low to high temperature. These three regions are also observed in the behaviour of the boron surface segregation coefficient (Auger data) which passes through a maximum near  $750^\circ\text{C}$  and in the evolution of the electrical properties (Hall effect). Defects in the epitaxial region consist mainly of stacking faults. As seen by Nomarski optical microscopy, their density ( $10^4\text{cm}^{-2}$  at the minimum for both orientations) as well as their size, strongly depend on the growth temperature.

All these observations are correlated in order to establish a global model of the boron incorporation during growth and to draw the conclusions on the capability of the technique to fabricate devices based on doped multilayered structures.

\* Present address: IBM, Thomas J. Watson Research Center.

## Intersubband Auger Recombination in Superlattice

*Peng-fei Yuh and K. L. Wang*

Device Research Laboratory  
Department of Electrical Engineering  
University of California, Los Angeles, CA 90024

### ABSTRACT

It is known that the recombination mechanism in narrow bandgap semiconductor lasers is dominated by the Auger process. An attempt to use the intersubband transitions in superlattice for laser is thus restricted by the Auger recombination process. The intersubband Auger recombination process is different from the conduction-to-valence band Auger since the subbands have different band structures, resulting in a different overlap integral and probability weighting function. The probability weighting function is comparable to that of the valence-to-conduction Auger process for narrow bandgap bulk material ( $\leq 0.3\text{eV}$ ). The overlap integral can be reduced by adjusting the miniband bandwidth. However, there is a tradeoff in controlling the bandwidth for a lower Auger rate (requiring narrower bandwidth) and for a larger carrier injection (requiring wider bandwidth). A closed form of the intersubband Auger rate is derived. It gives a much weaker bandgap and temperature dependence. Due to the adjustable overlap integral, the intersubband Auger rate can be made much lower than that of the conventional conduction-to-valence transition of the same bandgap.

PACS numbers: 79.20.Fv, 42.55.Px, 72.20.Jv, 73.40.Kp

8/12/87

*Sensitivity of the absorption edge to applied electric fields  
in GaAs-GaAlAs superlattices*

B. Jogai and K.L. Wang

*Device Research Laboratory, Department of Electrical Engineering, University of  
California, Los Angeles, California 90024*

**ABSTRACT**

The dependence of light absorption on an applied electric field in GaAs-GaAlAs superlattices is investigated theoretically for photon energies near the zero field bandgap. In the quantum well limit, the results show that while the red shift is negligible, the change in absorption with applied field for a given photon energy can be substantial. For nearly opaque barriers, the absorption coefficient at 100 kV/cm is about twice the zero field value. As the barriers become thinner, the red shift is enhanced but the sensitivity is diminished. At the same time the increased coupling between the wells gives rise to Franz-Keldysh oscillations.

Elemental and compound semiconductor devices today and beyond: influence of advanced epitaxial processes

Kang L. Wang

Electrical Engineering Department, University of California, Los Angeles  
405 Hilgard Avenue, Los Angeles, California 90024-1600

Abstract

This paper attempts to describe the advances of epitaxy of elemental and compound semiconductors and their impact on new physics, effects and applications of new devices. The impact of the recent epitaxy on material research is truly revolutionary. However, the scope is too immense to cover in a limited space and time. In lieu of the detailed descriptions of the epitaxial processes, I will try to highlight the most important substances of the advance. Several examples of newly discovered effects and new devices based on the artificially structured materials that are made possible by the advanced epitaxial techniques will be presented. These examples are by no mean exclusive and many other important ones are inadvertent omitted owing to the limited space and preferential interests of the author. Finally, some on-going research efforts as well as possible directions of further development of thin film epitaxy are discussed.

Introduction

The advance of epitaxy in semiconductors, particularly in molecular beam epitaxy, organometallic chemical vapor epitaxy, and other low temperature epitaxial processes have had a significant and perhaps an unprecedented impact on the new discoveries of the physical effects and phenomena as well as new devices.

This paper is to review the progress and the current status of epitaxy in semiconductor thin films. The possible new directions will also be discussed in the context of the industrial application of these technologies.

The revolutionary advance of epitaxy provides "opportunities of decades" in material research and the significances in material science and structured physics may be found for instance in the Report on Artificially Structured Materials.

Advance in epitaxial materials

The progress of the making of semiconductor materials as in other technologies in the human race is first to make good choice in utilizing some unique and special properties of the chosen material. For example in semiconductors, we had gone from Ge to Si and GaAs just like we had in utility materials from Cu to Fe and alloys. As we become good at it we begin the synthesis of new materials. With the advent of the new epitaxial processes, we are at the position of exercising the epitaxy control, i.e., engineering layered materials. In doing so we can grow at will the improved and new materials which could not be conceivably made before. More specifically, the advance of the epitaxial techniques make possible to fabricate improved heterojunctions and new superlattices and quantum well structures.

At present, there are many processes to grow semiconductor epitaxial layers. Among them, there are liquid phase epitaxy, chemical vapor epitaxy (CVD) or (low pressure CVD), molecular beam epitaxy and metal organic (or organometallic) chemical vapor deposition MOCVD or OMOCVD. Only CVD, MOCVD, and MBE will be discussed here as the progress is most evident in these areas. For these processes, the former three can be categorized as chemical processes and the last one as a physical process. In epitaxy, two conditions must be made in order to achieve high quality crystalline films in addition to the needed lattice match condition, which can be relaxed somewhat in low temperature strained layer growth. The two conditions are first to have an atomically clean surface prior to growth for seeding the epitaxial process and second to maintain a pure ambient during growth in order to reduce the undesired impurity level. The features of the two categories of epitaxial techniques are contrasted here not for the purpose of presenting the pros and cons but rather for assessing the future research directions. For MBE, a prior growth clean surface can be conveniently obtained and verified as all surface analysis tools can be made available readily. The ultra high vacuum condition also provides the desirable clean ambient during growth. The molecular flow can be interrupted without any observable delay, and atomically abrupt interface can always be attained if interface reactions are minimized. The deposition often occurs in a physical process and particle beams can

RHEED OBSERVATION OF MBE-GROWN  $\text{Ge}_x\text{Si}_{1-x}$  ON Si(111)

T.W.Kang, C.F.Huang, R.P.G.Karunasiri,

J.S.Park, C.H.Chern, and K.L.Wang

Device Research Laboratory

University of California

Los Angeles

Los Angeles, CA 90024-1600

**ABSTRACT**

Thin films of a  $\text{Ge}_x\text{Si}_{1-x}$  alloy with  $x = 0.5$  have been epitaxially grown using molecular beam epitaxy (MBE) on Si(111) substrates by simultaneous evaporation of Ge and Si. Surface reconstructions during the growth of  $\text{Ge}_x\text{Si}_{1-x}$  film were observed using reflection high energy electron diffraction (RHEED). A sharp  $7 \times 7 \rightarrow 5 \times 5$  transition of the RHEED pattern was observed. This is in agreement with the surface structures observed by LEED.

Abstract submitted  
for the March 1986 Meeting of the  
American Physical Society  
November 18, 1985

Sorting Category  
20b

Light Induced current in a GaAs/GaAlAs superlattice. B. Jogai and  
K.L. Wang, Dept. of Electrical Engineering, University of California at  
Los Angeles.\*

The superlattice is of interest as an optical detector since its  
electronic properties can be adjusted by changing the geometry. When an  
electric field is applied, the light induced current can be used to  
measure the intensity of the light. We have calculated the field-  
dependent absorption coefficient and the photo current for a GaAs/GaAlAs  
superlattice. Following Kane's approach [1], the field corrected  
wavefunctions are obtained from the zero field wavefunctions, and are  
then used to calculate the band to band tunneling current.

\*Supported by the Office of Naval Research.

1. E.O. Kane, J. Phys. Chem. Solids, 12, 181, 1959.



Signature of APS Member

K. L. Wang  
Same Name Typewritten  
7619 Boelter Hall, UCLA  
Los Angeles, CA 90024  
Address

## POLARITON STRUCTURE OF MULTILAYERED SEMICONDUCTING MATERIALS

J.P. Vigneron, A. Dereux, Ph. Lambin and A.A. Lucas  
Département de physique, Facultés Notre-Dame de la Paix  
61, rue de Bruxelles, B-5000 Namur, Belgium

S. Hecudains and M. Hannotiaux  
Centre d'Etude de l'Energie Nucléaire  
Boeretang 200, B-2400 Mol, Belgium

University of California, 7619 BH  
Los Angeles, Ca 90024, USA

Sharply defined multilayered structures have been grown from a variety of semiconducting materials. With these thin-film structures, the accumulation of interfaces gives rise to new excitation modes, that can be found both in the phonon and plasmon energy ranges. The detailed polariton structure of a general stratified structure, finite or infinite, and its effective dielectric response function can conveniently be assessed in terms of a new, Riccati-type initial value problem which can be used to quantitatively account for reflectance measurements, attenuated total internal reflection (ATR) and, using a non-retarded limit of the same formalism, electron energy-loss spectroscopy (HREELS).

The non-radiative excitations visible in ATR and HREELS experiments can be viewed as combinations of interacting interface modes. In the case of a semi-infinite superlattice, most of these mode evolve into continuous bands of Bloch states. Some others, mainly associated with the superlattice-vacuum interface evolve into isolated surface-like modes. New EELS experiments on GaAs-GaAlAs superlattices will be analyzed in the framework of this dielectric response description and recent measurements of the reflectivity of Si-Si<sub>x</sub>Ge<sub>1-x</sub> multilayered structures in the electronic excitation range will be presented and discussed.

**REFLECTION HIGH ENERGY ELECTRON DIFFRACTION OBSERVATION OF  
SUBSTRATE CLEANING DURING Si MOLECULAR BEAM EPITAXY**

C. F. Huang, R. P. G. Karunasiri, K. L. Wang, and T. W. Kang<sup>\*</sup>

Device Research Laboratory  
Electrical Engineering Department  
University of California  
Los Angeles, CA 90024-1600

**ABSTRACT**

The removal of the oxide on Si(100) surface resulting from the reaction with an impinging Si, Ge, or Ga beam on the substrate was investigated in Si molecular beam epitaxy (MBE) by reflection high energy electron diffraction (RHEED). The 2x1 reconstruction pattern due to the clean Si(100) surface was utilized in determining the optimum conditions for the cleaning methods used. It was found that all three beams can be effectively used for cleaning Si substrates as long as the proper parameters are chosen. In addition, a time dependent enhancement of the reconstruction pattern was observed after the Ge beam cleaning.

<sup>\*</sup> T. W. Kang was on leave from Dongguk University, Korea.

Abstract Submitted  
for the March 1987 Meeting of the  
American Physical Society

November 21, 1986

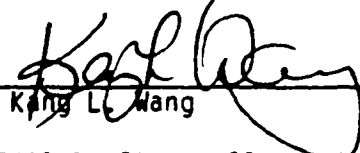
Sorting Category

20b

Electroabsorption in GaAs-GaAlAs Superlattices.\*

B. Jogai and K. L. Wang, Device Research Laboratory, UCLA. -- We have calculated the absorption coefficient in GaAs-GaAlAs superlattices in an applied electric field. Using the crystal momentum representation to represent the superlattice states, the transition rates between valence and conduction sub-bands are calculated for different values of the field. The band structure and unperturbed wave functions are obtained from a tight-binding model. The model allows for coupling between the sub-bands. Both the Franz-Keldysh effect and Franz-Keldysh oscillations emerge from the formalism. The absorption edge as a function of photon energy varies exponentially and has small oscillations superimposed on it. It is followed by a flat region characteristic of a two-dimensional electron gas.

\*Supported in part of the Office of Naval Research.

  
Kang L. Wang

7619 Boelter Hall, UCLA  
Los Angeles, CA 90024  
Address

## MBE GROWTH OF $\text{Ge}_x\text{Si}_{1-x}$ ON POROUS SILICON

C. H. Chern<sup>1</sup>, Y. C. Kao<sup>1</sup>, C. W. Neih<sup>2</sup>, G. Bai<sup>2</sup>, K. L. Wang<sup>1</sup>, and M-A. Nicolet<sup>2</sup>

<sup>1</sup> Device Research Laboratory, Electrical Engineering Department  
University of California, Los Angeles, CA 90024

<sup>2</sup> California Institute of Technology, Pasadena, CA 91125

### ABSTRACT

Recently, porous Si has been used as a patterned substrate for epitaxial growth of  $\text{CoSi}_2$  and GaAs. Encouraging results have been achieved in both cases although different concepts of the stress relief are applied.  $\text{Ge}_x\text{Si}_{1-x}$  can be grown onto Si pseudomorphically if the growth temperature is kept low and the thickness is restricted to below a "critical" thickness, which becomes thinner as the Ge composition gets larger. In this work,  $\text{Ge}_x\text{Si}_{1-x}$  with Ge compositions of 20%, 50% and 100% grown on both porous and single crystal Si are investigated. During the experiment, surface conditions were monitored by RHEED. TEM, RBS and the X-ray rocking curve technique were used for the characterization of samples. The results of strain relaxation and crystallinity of the  $\text{Ge}_x\text{Si}_{1-x}$  films are discussed.

### INTRODUCTION

Because of the increasing demand on very high speed and optoelectronic devices coupled with the vast existing Si technology in industry,  $\text{Ge}_x\text{Si}_{1-x}$  epitaxy on Si has aroused a great deal of interest in recent years. However, the up to 4.2% lattice mismatch between  $\text{Ge}_x\text{Si}_{1-x}$  and Si can cause a large density of misfit dislocations and thus cannot accommodate thick commensurate  $\text{Ge}_x\text{Si}_{1-x}$  layers. Several efforts, such as using strained layer superlattice buffer, rapid thermal annealing and tilted substrates[1-2] have been experimented to suppress the propagation of threading dislocations toward the  $\text{Ge}_x\text{Si}_{1-x}$  active region. All of these approaches have not given satisfactory results for decreasing the total defect density of the epitaxial layers.

Recently, a new approach for growing defect free epilayers on lattice mismatched substrates was proposed by Luryi et al.[3]. According to their theoretical calculation, a substrate having small seed pads of a lateral dimension about 10 nm is suggested to be used. This small size of seed pad is very difficult to fabricate by present lithography techniques. Porous Si substrates which have surface pads ranging from 3 to 20 nm have been developed as an alternative method. Current research on epitaxial growth of GaAs and  $\text{CoSi}_2$  on porous Si indicates that the porous Si substrate appears to be a promising substrate for improved epitaxial growth[4-5].

# ULTRAVIOLET LASER ASSISTED SILICON MOLECULAR BEAM EPITAXY

S.S. Rhee and K.L. Wang

Device Research Laboratory  
Electrical Engineering Department  
University of California at Los Angeles  
Los Angeles, California 90024

## Abstract

UV radiation effects on the surface cleaning,  $B_2O_3$  decomposition and Sb doping incorporation were studied by Auger electron spectroscopy, spreading resistance profiling and van der Pauw Hall measurement. 193 nm ArF laser and 248 nm KrF laser were used for UV sources. UV radiation was found to enhance the interdiffusion of Si and  $B_2O_3$ , Sb incorporation and the Hall mobility.

## Introduction

Pulsed UV lasers have been employed in photoenhanced MOCVD and it was successfully demonstrated that UV light irradiation improved the surface morphology, impurity concentrations and growth rate and lowered growth temperature (1-4). Most recently, UV laser has been introduced into the II-VI molecular beam epitaxy MBE as a new approach to control substitutional doping of II-VI compound semiconductors (5). It was shown that UV radiation greatly improves the electrical properties of the as grown II-VI epilayers. Another report on UV laser effect in III-V MBE area also showed a significant improvement of the film quality (6).

In MBE, irradiating the UV laser on the substrate can provide high energy with low momentum photons to the surface atoms and adlayer. Effects of UV laser radiation on the substrate can be photo-thermal effect caused by extremely high incident power or others such as increased surface mobility, decomposition of the surface constituents, modification of the bonds between bulk and surface species and modification of the electrical potential of the surface by generating photoexcited carriers.

In Si MBE, doping by coevaporation of Si and doping species suffers the drawbacks of low sticking coefficient of the dopant and long residence time. Several techniques have been developed to overcome these problems, namely potential enhanced doping or secondary ion implantation (7,8) and the electron irradiation enhanced doping technique (9). Both techniques significantly improved the incorporation as well as crystallinity and achieved sharp doping profiles for n-type Sb, but these techniques still suffer problems of having high residual defect density resulted from ion and electron impacts on the surface, especially at low substrate temperature. For p-type dopants, high vapor pressure boron oxide compound has been recently used to overcome the high temperature problem of pure boron source (10, 11). However substrate temperature has

## SURFACE RECONSTRUCTION OF MBE-GROWN $\text{Ge}_x\text{Si}_{1-x}$ ON Si(111)

C. F. Huang, R. P. G. Karunasiri, J. S. Park, K. L. Wang and T. W. Kang\*  
Device Research Laboratory, Electrical Engineering Department,  
University of California, Los Angeles, CA 90024-1600

\* T.W.Kang was on leave from Dongguk University, Korea.

### ABSTRACT

Surface reconstruction during the molecular beam epitaxy (MBE) growth of  $\text{Ge}_x\text{Si}_{1-x}$  ( $x = 0.2 - 1.0$ ) film on Si(111) was studied using reflection high energy electron diffraction (RHEED). A series of reconstruction pattern transitions was observed due to the formation of strain layer and its relaxation. The critical thickness obtained using the thickness of the  $\text{Ge}_x\text{Si}_{1-x}$  film at the transition of the reconstruction pattern agrees well with the previously reported values. The strain dependence of RHEED patterns for  $\text{Ge}_x\text{Si}_{1-x}$  film was substantiated by Raman scattering.

### I. INTRODUCTION

The growth of  $\text{Ge}_x\text{Si}_{1-x}$  thin films on silicon has received increasing attention in recent years [1-3]. Although progress has made it possible to grow high-quality pseudomorphic Si/ $\text{Ge}_x\text{Si}_{1-x}$  multilayer structures [1], the initial stage of growth of  $\text{Ge}_x\text{Si}_{1-x}$  thin films and their surface structures still remains relatively unknown. This motivated us to investigate the surface reconstruction of  $\text{Ge}_x\text{Si}_{1-x}/\text{Si}(111)$  during growth using RHEED. In this paper, we described the use of RHEED for the determination of critical thickness of  $\text{Ge}_x\text{Si}_{1-x}$  films on Si(111).

Surface reconstructions of  $\text{Ge}_x\text{Si}_{1-x}/\text{Si}(111)$  films after growth have been examined [4-7] using low energy electron diffraction (LEED). A  $7 \times 7$  LEED pattern was observed by Gossmann et al. [4] for thin films ( $\sim 65 \text{ \AA}$ ) of Ge grown by MBE on Si(111) substrate and the  $\text{Ge}_{0.5}\text{Si}_{0.5}$  film clearly showed a  $5 \times 5$  LEED pattern. Furthermore, McRae [5] and Shoji et al. [6] studied the epitaxy of Ge on Si(111) vicinal surfaces and observed the formation of  $5 \times 5$  LEED patterns after annealing. Our previous RHEED studies [8] showed a sharp  $7 \times 7 \rightarrow 5 \times 5$  transition for  $\text{Ge}_{0.5}\text{Si}_{0.5}/\text{Si}(111)$  within the critical thickness, which is in agreement

# Strain Distribution of MBE Grown $\text{Ge}_x\text{Si}_{1-x}/\text{Si}$ Layers by Raman Scattering\*

S. J. Chang, M. A. Kallel and K. L. Wang  
Device Research Laboratory, Electrical Engineering Department  
University of California, Los Angeles, CA 90024

R. C. Bowman, Jr.  
The Aerospace Corporation  
M1-109, P. O. Box 92957, Los Angeles, CA 90009

The successful growth of  $\text{Ge}_x\text{Si}_{1-x}/\text{Si}$  strained layer superlattice (SLS) by molecular beam epitaxy has recently stimulated considerable interest. The bandgap engineering of such a system has led to some potentially useful photonic and electronic applications. A lot of work has been done to gain a better understanding of the structure. Raman scattering technique has been particularly useful.

It is known that dislocation free  $\text{Ge}_x\text{Si}_{1-x}$  overlayers may only be grown up to a certain critical thickness  $h_c$  depending on the alloy composition fraction  $x$  and the growth temperature [1]. For  $\text{Ge}_x\text{Si}_{1-x}/\text{Si}$  multilayers, strain condition will depend on the choice of the buffer layer and the overall superlattice thickness.

The objective of this paper is to study the strain distribution in the superlattice as a function of alloy composition and the distance from the interface using the technique of Raman scattering. Although  $\text{Ge}_x\text{Si}_{1-x}/\text{Si}$  structures have been previously studied by Raman, the focus was mainly on determining stress and critical thickness [1][2][3]. In our work, we are dealing with thick structures and our goal is to determine the distribution of strain close to the interface. Also, in addition to using regular Si for the substrate, we are trying to use porous Si as well.

The experiment was performed at room temperature in the near back scattering geometry. The samples were excited with a Spectra Physics 2020 Argon ion laser operated at 5145Å, and analyzed with a Spex 1404 double spectrometer and an EG&G 941 photon counter. Fig. 1. is a typical Raman spectrum for a thick  $\text{Ge}_{0.5}\text{Si}_{0.5}/\text{Si}$  SLS on Si substrate. Because of the

\*Submitted to SPIE meeting Spring 1988.

thick superlattice, the laser beam cannot reach the substrate and only 4 peaks were observed. The peaks ascribed to the vibrations of Ge-Ge, Ge-Si, and Si-Si bonds from the  $\text{Ge}_{0.5}\text{Si}_{0.5}$  layers were all clearly shifted upward due to the lateral compression strain, and the peak ascribed to the Si optical mode originating from the Si layers was shifted downward as a result of lateral tensile strain.

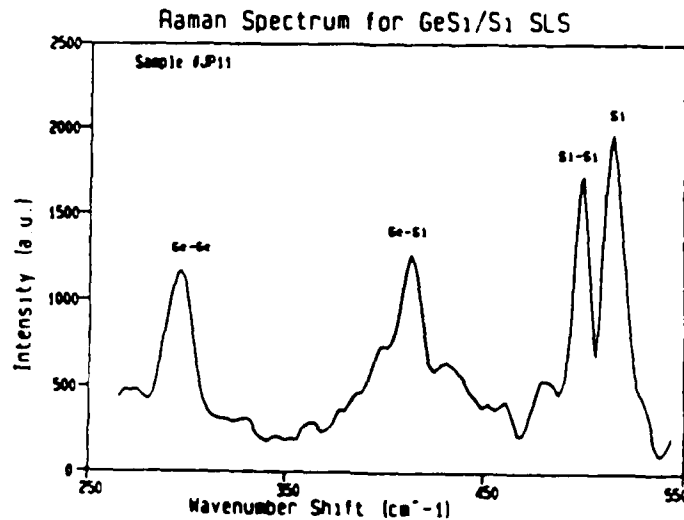


Fig. 1. Raman spectrum for a  $\text{Ge}_{0.5}\text{Si}_{0.5}/\text{Si}$  SLS

In order to study the crystal properties of the layers close to the interface of the thick  $\text{Ge}_x\text{Si}_{1-x}/\text{Si}$  SLS, a small angle bevel was made by using angle lapping, as shown in Fig. 2 [4]. The laser light was focused to a small spot and the Raman spectra were obtained by successively moving the sample in the direction perpendicular to the bevel edge with a micrometer. With the known bevel angle and the distance between the focused laser light and the bevel edge, the effective thickness of the laser probing position could be calculated.

Different samples were grown and compared, strain distribution as a function of the distance from the interface was obtained for thick  $\text{Ge}_x\text{Si}_{1-x}/\text{Si}$  SLS's and comparisons with thin

structures were made. A qualitative understanding of lattice crystallinity was also assessed from the FWHM of the Raman peaks. The preliminary results for superlattices grown on porous Si are inconclusive at this point. However, it is expected that shifts should be different from the case of regular Si since porous Si effectively provides a patterned substrate for relaxing the strain in the growth.

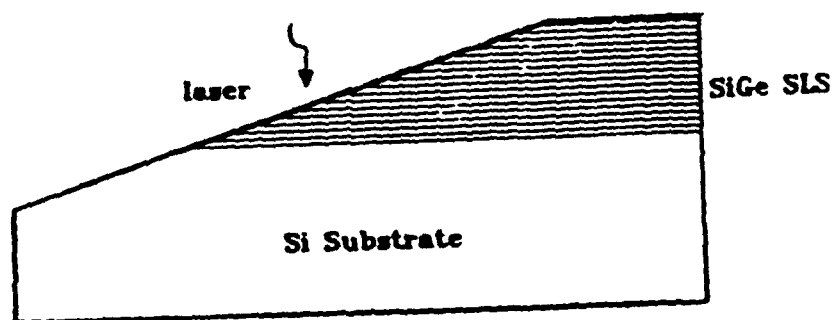


Fig. 2. Small angle bevel and laser probing

**References :**

1. R. People, IEEE Trans. Quantum Electronics, Vol. E-22, p1696, 1986
2. G. Abstreiter, H. Brugger, T. Wolf, Phys. Rev. Lett. Vol 54, p2441, 1985
3. R. People, J. C. Bean, D. V. Lang, J. Vac. Sci. Technol. Vol. A3, p846, 1985
4. Y. Huang, P. Y. Yu, M. Charasse, Y. Lo, S. Wang, Appl. Phys. Lett. Vol. 51, p192, 1987

\*This work is in part supported by the Office of Naval Research and the Army Research Office

END  
DATE  
FILMED

4-88

DTIC